


RESEARCH

Open Access



# The therapeutic use of clonal neural stem cells in experimental Parkinson's disease

Anna Nelke<sup>1,2,3\*</sup> , Silvia García-López<sup>1,2,3</sup>, Javier R. Caso<sup>4</sup> and Marta P. Pereira<sup>1,2,3\*</sup>

## Abstract

**Background** Parkinson's disease (PD), the second most common neurodegenerative disease in the world, is characterized by the death or impairment of dopaminergic neurons (DAN) in the substantia nigra pars compacta and dopamine depletion in the striatum. Currently, there is no cure for PD, and treatments only help to reduce the symptoms of the disease, and do not repair or replace the DAN damaged or lost in PD. Cell replacement therapy (CRT) seeks to relieve both pathological and symptomatic PD manifestations and has been shown to have beneficial effects in experimental PD models as well as in PD patients, but an apt cell line to be used in the treatment of PD has yet to be established. The purpose of this study was to examine the effects of the transplantation of hVM1 clone 32 cells, a bankable line of human neural stem cells (hNSCs), in a PD mouse model at four months post-transplant.

**Methods** Adult (five month-old) C57BL/6JRcchsd male mice were injected with 1-methyl-4-phenyl-1,2,3,6-tetrahydropyridine and subsequently transplanted with hVM1 clone 32 cells, or buffer, in the left striatum. Four months post-transplant, behavioral effects were explored using the open field and paw print tests, and histological analyses were performed.

**Results** Transplantation of hVM1 clone 32 cells rescued dopaminergic nigrostriatal populations in adult Parkinsonian mice. Motor and neurological deterioration were observed in buffer-treated mice, the latter of which had a tendency to improve in hNSC-transplanted mice. Detection of mast cell migration to the superficial cervical lymph nodes in cell-transplanted mice denoted a peripheral effect. Transplantation of hNSCs also rescued neuroblast neurogenesis in the subgranular zone, which was correlated with dopaminergic recovery and is indicative of local recovery mechanisms.

**Conclusions** In this proof-of-concept study, the transplantation of hVM1 clone 32 cells provided neuroprotection in adult Parkinsonian mice by restoring the dopaminergic nigrostriatal pathway and hippocampal neurogenesis, demonstrating the efficacy of cell replacement therapy as a treatment for PD.

**Keywords** Cell replacement therapy, Human neural stem cell, Neurotrophic factor, Parkinson's disease

\*Correspondence:

Anna Nelke  
anna.nelke@dpag.ox.ac.uk  
Marta P. Pereira  
pereiram@cbm.csic.es

<sup>1</sup>Unit of Molecular Neuropathology, Physiological and pathological processes Program, Centro de Biología Molecular Severo Ochoa UAM-CSIC, Calle Nicolás Cabrera, 1, Madrid 28049, Spain

<sup>2</sup>Department of Molecular Biology, Faculty of Science, Universidad Autónoma de Madrid, Ciudad Universitaria de Cantoblanco, Madrid 28049, Spain

<sup>3</sup>Institute for Molecular Biology – IUBM (Universidad Autónoma de Madrid), Madrid, Spain

<sup>4</sup>Department of Pharmacology and Toxicology, School of Medicine, Universidad Complutense de Madrid, Centro de Investigación Biomédica en Red de Salud Mental, Instituto de Salud Carlos III (CIBERSAM, ISCIII), Instituto de Investigación Sanitaria Hospital 12 de Octubre (Imas12), Instituto Universitario de Investigación Neuroquímica (IUIN-UCM), Avda. Complutense s/n, Madrid 28040, Spain



© The Author(s) 2024. **Open Access** This article is licensed under a Creative Commons Attribution-NonCommercial-NoDerivatives 4.0 International License, which permits any non-commercial use, sharing, distribution and reproduction in any medium or format, as long as you give appropriate credit to the original author(s) and the source, provide a link to the Creative Commons licence, and indicate if you modified the licensed material. You do not have permission under this licence to share adapted material derived from this article or parts of it. The images or other third party material in this article are included in the article's Creative Commons licence, unless indicated otherwise in a credit line to the material. If material is not included in the article's Creative Commons licence and your intended use is not permitted by statutory regulation or exceeds the permitted use, you will need to obtain permission directly from the copyright holder. To view a copy of this licence, visit <http://creativecommons.org/licenses/by-nc-nd/4.0/>.

## Background

Parkinson's disease (PD) is the second most common neurodegenerative disease in the world and the most common movement disorder for which there is presently no cure. Furthermore, the majority of PD cases are termed idiopathic or sporadic, thus having no known cause. Parkinson's disease is characterized by the death or impairment of dopaminergic neurons (DAN) in the substantia nigra pars compacta (SNpc) and the depletion of dopamine (DA) in the striatum (Str). The loss of DAN in the SNpc leads to the decrease of DA in the Str as DAN project to the Str. It is this pathology that causes the motor symptoms, such as tremors, rigidity, bradykinesia, and postural instability, that are observed in PD patients [1–4].

In addition to the reduction of tyrosine hydroxylase (TH) expression in the SNpc and Str, as well as the presence of Lewy bodies in the brain, the loss of neurotrophic factors (NTFs) is another hallmark of PD. In the SNpc of PD patients, levels of glial cell-derived neurotrophic factor (GDNF) and brain-derived neurotrophic factor (BDNF) are decreased [5–7]. Moreover, GDNF specifically increases the survival, proliferation, differentiation, and migration of DAN, and increases the expression of DAN-associated genes, while BDNF promotes neurite outgrowth in DAN and regulates hippocampal neurons, thus being important for synaptic plasticity, learning, and memory [5, 8–12]. Besides GDNF and BDNF, other factors, namely fractalkine (FKN), stem cell factor (SCF), vascular endothelial factor A (VEGF-A), and vascular endothelial factor C (VEGF-C), have also been shown to play a protective role for DAN in basal and experimental PD conditions [13–22].

Although there is a plethora of treatments available for PD such as DA restoring medications, none of them are effective in the long-term and they only treat the symptoms of the disease, failing to address the underlying issue that is the loss of DAN, as they do not replace or repair the DAN lost or damaged, respectively, in PD [2, 7, 23]. Therefore, with other current treatments not fulfilling all requirements to improve the patient's life, the goal of PD treatment becomes cell replacement. In recent years, cell replacement therapy (CRT) has come to the forefront of science with its potential to treat diseases such as PD, using various cell sources such as human induced pluripotent stem cells, human mesenchymal stem cells and human neural stem cells (hNSCs). Several clinical trials have demonstrated promising results, where PD patients showed motor improvement for many years post-transplant and post-mortem, surviving TH+grafted cells were found in the patients' brain. As well, there are currently multiple ongoing clinical trials assessing CRT in PD patients [23–28]. With all of this potential, there are some concerns with CRT that need

to be addressed such as ethical issues behind the acquisition of tissue needed for some cell types, immunosuppression of treated patients, graft-induced dyskinesias, patient heterogeneity in that not every patient is responsive to CRT, and the standardization of methods of cell transplantation including amount of cells transplanted as well as location of grafts [7, 23, 26].

One hNSC line that has so far only been used in experimental PD models is the hVM1 clone 32 cell line. These fetal-derived hNSCs demonstrate true A9 DAN characteristics upon differentiation in vitro and induce behavioral improvement upon transplantation in Parkinsonian rats and middle-aged Parkinsonian mice [29, 30]. The latter study showed that the dopaminergic cells and fibers in the nigrostriatal pathway were not significantly restored by hNSC transplant in older animals, consistent with the reduced endogenous capacity of recovery in aging. Thus, it is pertinent to test the outcome and effectivity of CRT using the hVM1 clone 32 cells in adult Parkinsonian mice which retain a greater ability to trigger recovery and plasticity mechanisms compared to older animals. Therefore, in this study, hVM1 clone 32 cells were transplanted in a 1-methyl-4-phenyl-1,2,3,6-tetrahydropyridine (MPTP) PD mouse model in order to see if the transplanted hNSCs could replace and take over the functions of the lost or impaired DAN by integrating in the host environment, thus rescuing nigrostriatal innervation, improving motor deficits, and exerting neurotrophic effects.

## Methods

### Ethics statement

All animal work and use of hNSCs were approved by and adhered to the guidelines of the Universidad Autónoma de Madrid (CEI 62-1077-A079; 06/03/2015) and the Comunidad de Madrid (PROEX149/15; 29/05/2015) Research Ethics Committees, both with project title "Desarrollo hacia la clínica del trasplante de células troncales neurales humanas para la enfermedad de Parkinson". Details about the human fetal origin of the hVM1 clone 32 cells used in this study, including consent and donors, can be found in previous articles describing these cells [29, 31]. Animal procedures were performed at the Animal Facility of the Centro de Biología Molecular Severo Ochoa. All animal experiments complied with the ARRIVE guidelines and were carried out in accordance with the EU Directive 2010/63/EU for animal experiments guidelines. All efforts were made to minimize animal suffering and to reduce the number of animals used by monitoring weight as well as signs of pain and distress.

### Cell culture

The cells used in this study were hVM1 clone 32, with details previously described [29, 31]. Briefly, it is a clone isolated based on increased TH generation from the

stable, *v-myc*-immortalized hVM1 cell line. The hVM1 cells were generated from dissociated tissue of the ventral mesencephalon of a 10 week-old aborted human fetus. The hVM1 clone 32 cell line is a unique biological material developed by the laboratory in 2009 and was authenticated by STR profile analysis [29, 31].

Cells were routinely cultured on plastic plates treated with 10 µg/ml polylysine (Sigma-Aldrich P1274) in proliferation medium. The proliferation medium composition was as follows: The base was Dulbecco's modified Eagle's medium/F-12, GlutaMAX supplement medium (Gibco 31331028), 1% AlbuMAX (Gibco 11020021), 50 mM HEPES (Gibco 15630106), and 0.6% D-glucose (Merck 104074). To this, 1X N2 supplement (Gibco 17502048), 1X homemade non-essential amino acids (composed of L-alanine, L-asparagine, L-aspartic acid, L-glutamic acid, and L-proline, all with a final concentration of 0.4 mM), 100 U/ml penicillin, 0.1 mg/ml streptomycin, 20 ng/ml human recombinant fibroblast growth factor 2 (R&D systems 233-FB), and 20 ng/ml human recombinant epidermal growth factor (R&D systems 236-EG), were added. Cells were grown at 37 °C, in a 95% humidity, 5% CO<sub>2</sub>, and 5% O<sub>2</sub> atmosphere. For differentiation experiments, multiwell plates were treated with 30 µg/ml polylysine overnight, and then incubated with laminin (Sigma-Aldrich L2020) at 5 µg/ml for 5 h, before seeding cells into wells. Cells were seeded at 20,000 cells/cm<sup>2</sup>, in proliferation medium. Twenty-four hours later, this medium was replaced with differentiation medium, which is the same one used for proliferation experiments, but the growth factors are replaced with 2 ng/ml human recombinant GDNF (Peprotech 450-10) and 1 mM dibutyryl cAMP (Sigma-Aldrich D0627) [32]. One day later, the differentiation medium was fully changed, and after this, two thirds of the differentiation medium was changed every two days. Differentiated cell samples were collected after seven days of differentiation. Equivalent multiwell plates with proliferation medium were seeded in parallel and these samples were collected at three days post-seeding.

#### Animal procedures

Male C57BL/6J RccHsd mice (Envigo, Netherlands) were used in this study. Animals were five months old with an average weight of 34.1 g at the beginning of the experiment, and all mice were housed in a temperature- and humidity-controlled room on a 12-hour light/dark cycle and fed *ad libitum* with standard food and water. Animals were randomly separated into one of three experimental groups: Control, MPTP+buffer, and MPTP+cell. Animals arrived from the supplier in groups of three or four mice, and these cages were randomly assigned to one of the three experimental groups. Potential confounders were minimized using randomization, and

consistency in as many factors as possible (i.e. age, sex, genotype, handling) of all mice. Control mice were injected i.p. with 0.9% saline once every two hours, with a total of three injections, at 10 µl/g. Using the same injection protocol, PD was induced in other mice by injecting MPTP (Sigma-Aldrich M0896) i.p. at 15 mg/kg. The dose of 15 mg/kg was chosen in order to have less nigrostriatal damage before the transplant thus mimicking an intermediate stage of PD, since it has been shown that when MPTP is administered at 18 mg/kg or 20 mg/kg once every two hours, with a total of four injections, there is a great loss of TH+ fibers and cells in the Str and SNpc, respectively [33]. During pilot studies, a very high percentage of mice died after the fourth injection and therefore, it was decided that only three injections would be made. Mortality rate was 9% following MPTP injections. One week later, mice injected with MPTP underwent stereotaxic surgery to receive an intracerebral injection in the left Str (Coordinates from Bregma: Anteroposterior 0.25 mm, Mediolateral 2.75 mm, Dorsoventral 3 mm) of either 1.5 µl transplantation medium (MPTP+buffer group) or 100,000 mycoplasma-free, undifferentiated hVM1 clone 32 cells in passage 26 in 1.5 µl transplantation medium (MPTP+cell group). The timepoint of one week was used because it has been reported that after one week, the loss of DAN in the SNpc is stable [33]. The transplantation medium was composed of the following: 49% Leibovitz's L-15 Medium (ThermoFisher Scientific 11415064), 49% filtered 0.6% Glucose (Merck 104074) in 1X PBS, and 2% B-27 Serum-Free Supplement (Gibco 17504044). The transplantation medium is different than the proliferation medium and contains Leibovitz's L-15 Medium so that the hVM1 clone 32 cells are nourished while transitioning from in vitro to in vivo in an unstable environment in terms of temperature as well as O<sub>2</sub> and CO<sub>2</sub> levels, and to make sure that these hNSCs are not dividing which could cause tumor growth upon transplantation into the mouse brain.

For surgery, animals were anesthetized with a mixture of ketamine (Merial) at 80 mg/kg and xylazine (Calier) at 10 mg/kg injected i.p. When animals were confirmed to be asleep via toe pinching, surgery began. After positioning the animal's head in the frame of the stereotaxic apparatus, the animal's skull was revealed and a 23-gauge needle with 0.635 mm outer diameter was used to make a hole in the skull. Through this hole, a 22-gauge needle (Hamilton Company; 22 gauge, Small Hub RN NDL, length 0.75 in, point style 4 cut at an angle of 10–12°) held in the attached syringe (Hamilton Company; 10 µl, Model 701 RN, 26s gauge, 51 mm, point style 2) was lowered into the brain to inject either the transplantation medium or hNSCs in the left Str. The speed of injection was 1 µl/min, and the needle was left in for 2 min after injecting cells before its slow removal. The antibiotic

oxytetracycline (0.2 mg/ml; Terramycin®, Zoetis) was delivered *ad libitum* in the drinking water of MPTP-treated animals starting the day of surgery for a total period of one week as a preventative measure. In order to avoid graft rejection, two days before the transplants and for the first week post-transplant, all animals were given an i.p. injection of cyclosporine A (CSA; Novartis) at 10 mg/kg once daily. For the remainder of the experiment, all animals were treated with daily weekday i.p. injections of CSA at 10 mg/kg, and twice a week, CSA was included in the drinking water, prepared with the following components: 0.25 g/L CSA and sweetener. All animals survived both buffer and hNSC transplant surgeries, and showed no symptoms of distress, infection, or pain. Mice were sacrificed at either one or four months post-transplant.

### Behavioral tests

In order to detect neurological and motor alterations, animals were subjected to the open field test (OFT) and paw print test (PPT) [34, 35]. Animals received three training sessions prior to taking basal measurements for all behavioral tests. All OFTs were performed in the same room, with the same lighting, and at the same time.

### OFT

Animals were placed in a 40 cm x 40 cm x 30 cm (L x W x H) four-walled cubic box and their movements were filmed for 10 min. Time spent in the center (20 cm x 20 cm central area), distance travelled, time spent grooming (mouse licks or scratches itself while stationary), time spent rearing (mouse stands on hind legs), urination (number of puddles or streaks of urine), and defecation (number of fecal boli), were measured using the ANY-maze behavioral tracking software (Stoelting Europe).

### PPT

The animals' paws were painted (forelimbs in green and hindlimbs in orange) and the mice then walked on a 40 cm x 12 cm white piece of paper. Contralateral (CL) and ipsilateral (IL) stride length (the distance between two same-sided forelimbs or two same-sided hindlimbs), and CL-IL and IL-CL stride width (the distance between two opposite-sided forelimbs or two opposite-sided hindlimbs), were measured.

### Immunohistochemistry

The animals were euthanized by CO<sub>2</sub> inhalation by gradual air displacement in a euthanasia chamber with compressed CO<sub>2</sub>. Post-mortem transcardial perfusion was carried out with saline buffer and fixation was done using cold 4% paraformaldehyde. After 12-hour post-fixing with 4% paraformaldehyde, the tissue was dehydrated in 30% sucrose until the tissue sank. Free-floating

15 µm-thick coronal sections of the brain were sliced using a freezing microtome.

Brain sections were washed and then blocked in 3–5% serum in 1X PBS/0.3% TritonX-100 and incubated with primary antibody in 1% serum in 1X PBS/0.3% TritonX-100 at 4°C overnight. The following primary antibodies were used: TH (1:400; Pel-Freez P40101-150), glial fibrillary acidic protein (GFAP) (1:1000; DAKO Z0334), ionized calcium-binding adapter molecule 1 (Iba1) (1:1000; Wako 019-19741), nestin (NES) (1:300; Novus Biologicals NB100-1604), Ki-67 (1:100; ThermoFisher Scientific RM-9106-S1), doublecortin (DCX) (1:300; Santa Cruz sc-8066), STEM121 (1:500; Takara Bio Y40410), BDNF (1:400; Abcam ab108319), and FKN (1:200; Abcam ab25088). Sections stained with TH and DCX were incubated with a mix of 1% of 30% hydrogen peroxide, 3% methanol, and 6% 1X PBS for 15 min, before blocking, and DCX sections were incubated with 1% SDS in 1X PBS for 5 min prior to the latter step. Sections in BDNF and FKN immunostainings were incubated with citrate buffer (pH 6.0; 10mM citric acid; Santa Cruz sc-214745) for 30 min and washed prior to blocking.

The next day, TH- and DCX-stained sections were incubated with appropriate biotinylated secondary antibodies (Biotinylated Goat Anti-Rabbit IgG Antibody (1:500; Vector Laboratories BA-1000) and Biotinylated Horse Anti-Goat IgG Antibody (1:200; Vector Laboratories BA-9500)), washed, incubated in ABC solution (VECTASTAIN Elite ABC HRP Kit, Vector Laboratories PK-6100), washed, and developed with the Vector VIP Peroxidase (HRP) Substrate kit (Vector Laboratories SK-4600). Samples were then mounted onto glass slides (Menzel-Gläser), air-dried, dehydrated with xylene, and coverslipped with distyrene, plasticiser, and xylene mounting medium.

After primary antibody incubation, fluorescent immunohistochemistry samples were washed and incubated with adequate secondary antibodies and 4',6-diamidino-2-phenylindole (1:1000; Santa Cruz sc-3598), in 1% serum in 1X PBS/0.3% TritonX-100 at RT for 2 h. The following secondary antibodies were used: Goat anti-Rabbit IgG (H+L) Highly Cross-Adsorbed Secondary Antibody, Alexa Fluor 546 (1:400, 1:500, or 1:1000; Invitrogen A-11035), Goat anti-Rabbit IgG (H+L) Highly Cross-Adsorbed Secondary Antibody, Alexa Fluor 488 (1:1000; Invitrogen A-11034), Alexa Fluor 488 AffiniPure Donkey Anti-Chicken IgY (IgG) (H+L) (1:500; Jackson ImmunoResearch 703-545-155), and Goat anti-Mouse IgG (H+L) Highly Cross-Adsorbed Secondary Antibody, Alexa Fluor 488 (1:1000; Invitrogen A-11029). All fluorescent immunostaining samples were washed, mounted onto glass slides (Menzel-Gläser), air-dried, and coverslipped with homemade Mowiol mounting medium,

composed of 10% MOWIOL 4–88 Reagent (Merck 475904).

### **Toluidine histology**

Ten  $\mu\text{m}$ -thick sections of superficial cervical lymph nodes (LNs) were sliced onto glass slides (Menzel-Gläser) using a cryostat, while free-floating brain sections were mounted onto glass slides (Menzel-Gläser) prior to staining. Slides containing brain and LN samples were stained with acidic toluidine blue working solution. The working solution was prepared as follows: 5 ml toluidine blue stock solution (1% toluidine blue O (Sigma-Aldrich T3260) in 70% ethanol), and 45 ml 1% NaCl (Merck Millipore 7647-14-5) in  $\text{dH}_2\text{O}$  (pH 2.27). After, slides were dehydrated with ethanol, cleared in xylene, and cover-slipped with distyrene, plasticiser, and xylene mounting medium.

### **Luminex assay**

Proliferation and differentiation conditioned media (CM) were collected from their respective plates and centrifuged at 2500 rpm at RT for 10 min. Supernatant was collected and stored at  $-80^\circ\text{C}$  for further analysis. Proliferation and differentiation CM, along with 20/20+ (proliferation) and Lotharius (differentiation) media, were analyzed with the Luminex Human Magnetic Assay custom-made plate (Bio-technie R&D Systems) for the following analytes: BDNF, FKN, GDNF, SCF, VEGF-A, and VEGF-C. These analytes were chosen based on PD pathogenesis and treatment literature. Observed concentration (pg/ml) of two replicates of each sample were measured using the Bio-Rad Bio-Plex 100 system.

### **Microscopy**

Images of TH, toluidine, and DCX stainings, as well as representative brightfield images, were obtained with an Axioskop 2 Plus microscope (Zeiss), DMC6200 camera (Leica), and LAS software (Leica), using the 2.5X, 5X, and 10X objectives. Nestin and Fig. 7 images were obtained with a DM IRB microscope (Leica), DC100 camera (Leica), and LAS software (Leica), using the 20X and 40X objectives. If necessary, images of all of the aforementioned stainings were then automatically merged using Adobe Photoshop CS5 Extended. All GFAP and Iba1 images were obtained with the Tile Scan of an Axiovert 200 microscope (Zeiss), pco.edge camera (PCO), and MetaMorph software (Molecular Devices), using the 20X objective. Images of striatal BDNF and FKN immunostainings as well as all representative fluorescent images, except for those in Fig. 7, were obtained with a LSM800 confocal microscope (Zeiss) with two GaAsP detectors and ZEN Blue software (Zeiss), using the 10X, 20X, and 40X objectives. For each staining of a specific region, all image parameters (i.e. exposure time, gamma, resolution,

pin hole) were the same for all images of all samples. Investigators were blinded to group assignment during image acquisition.

### **Histological quantifications**

Anteroposterior coordinate ranges from Bregma for the quantified sections were 0.98 to 0.38 mm for the rostral Str and subventricular zone (SVZ),  $-0.46$  to  $-0.82$  mm for the caudal Str,  $-2.80$  to  $-3.64$  mm for the SNpc, and  $-1.46$  to  $-2.06$  mm for the subgranular zone (SGZ) [36]. For TH, GFAP, Iba1, and DCX (SGZ), immunostainings, region of interest was drawn, threshold was set to be the same for all animals for each immunohistochemistry, and area fraction was measured. For TH immunostainings, the area fraction in the Str was made up of fibers and that of the SNpc was made up of cells and their prolongations. After taking photos of LNs, area was measured and number of mast cells (MCs) was counted manually. For DCX and NES quantifications in the SVZ, after setting threshold, immunopositive area was measured. For Iba1 cell morphological analysis, cell soma size and roundness were quantified as described in Davis et al. [37]. ImageJ/Fiji was used to do all quantifications except that of Ki-67. The number of Ki-67+ cells in the SVZ was counted by an unbiased observer with a DM IRB microscope (Leica) using the 20X objective. Two-five sections, including both IL and CL sides, of each animal from every experimental group were quantified, and all three experimental groups were tested at once in order to allow for comparison. Investigators were blinded to group assignment during histological quantifications.

### **Statistical analysis**

A total of 18 mice were used for the animal experiments and stainings analyzed at one month post-transplant. Two replicates of the animal experiments and stainings analyzed at four months post-transplant were performed, with a total of 30 animals used in the first replica and 27 animals used in the second replica. Similar tendencies were observed in both replicas. The results and statistics from four months post-transplant presented in this article are from the second replica, except for time spent in center in the OFT, LN size, and DCX expression in the SVZ, which are based on combined quantifications from the two replicas. A minimum of four animals per experimental group were used in all one- and four-month post-transplant replicas. No sample size calculation was performed; sample sizes were chosen based on previous *in vivo* experiments done in the laboratory to allow for statistical power and to comply with the 3Rs (Replacement, Reduction, and Refinement) by reducing the number of animals used. For the Luminex assay, a minimum of three proliferation and seven differentiation CM samples, from at least three independent experiments, were

analyzed. Exact *n* used for each experiment is indicated in the figure legends. For each quantification performed, measurements were taken from distinct samples, thus *n* expresses the total number of biological replicates. All figures were made and all statistical analyses were done using GraphPad Prism 7. Graph columns represent mean values, with individual data points shown with circles, while error bars indicate standard error of the mean. In Fig. 6c, the graphs illustrate the linear regression line with XY paired data points shown with circles. For comparisons between more than two groups, one-way analyses of variance (ANOVAs) followed by Tukey's multiple comparisons post-hoc test were performed in order to compare the mean of each column with the mean of every other column. To show linear correlation in Fig. 6c, the Pearson correlation coefficient (*r*) was calculated with a two-tailed *P* value. For comparisons between two groups, as in the case of the Luminex assay in Fig. 8a, two-tailed unpaired *t*-tests were performed. Some data were excluded for various reasons. Among them, outliers, mice stopping in the middle of the paper in the PPT, striatal slices with glial scar around the needle mark, and damaged or ripped tissue. These criteria were not established a priori. For all statistical tests, a *P* value of less than 0.05 was considered statistically significant. Investigators were aware of group allocation during allocation and conduct of experiment, but blinded to group allocation during outcome assessment and data analysis.

## Results

### Nigrostriatal pathway degeneration and recuperation

A cohort of mice from the three experimental groups was sacrificed one month post-transplant in order to analyze TH immunoreactivity in the nigrostriatal pathway to verify that the experimental model and transplantation were working short-term. Mouse brains were analyzed for TH immunoreactivity in the Str and SNpc, the two main regions affected in PD. In the rostral Str, the level of the Str closer to the site of the transplant, there was an 88% decrease in TH+area in buffer-transplanted animals compared to controls ( $P < 0.0001$  for IL and  $P < 0.0001$  for CL). Mice transplanted with hNSCs showed a 76% increase in TH+fibers compared to those treated with buffer ( $P = 0.0019$  for IL and  $P = 0.0176$  for CL). Controls had 50% more striatal TH expression than hNSC-treated animals ( $P = 0.0009$  for IL and  $P = 0.0004$  for CL) (Fig. 1a left). In the SNpc, TH immunoreactivity in buffer-treated mice decreased by 68% compared to control animals ( $P < 0.0001$  for IL and  $P < 0.0001$  for CL). Compared to buffer-treated mice, there was an increase in nigral TH expression upon hNSC transplantation, 57% on the IL side and 40% on the CL side, attaining significance on only the IL side ( $P = 0.0063$ ). Similar to the rostral Str, controls had an increased TH+area in the SNpc

compared to hNSC-transplanted mice, 26% on the IL side and 48% on the CL side, although this was significant on only the latter side ( $P = 0.0002$ ) (Fig. 1a right).

For the main experiment, the endpoint of four months post-transplant was chosen in order to explore the effects of the transplant more long-term to see if the nigrostriatal improvements continued past one month post-transplant. Also, it has been reported that CSA, used to immunosuppress the mice in order to avoid graft rejection, can cause damage to the mice's health long-term and can only be administered for a maximum of 18–20 weeks, or 4.5–5 months [38, 39]. Four months post-transplant, analysis of TH+fibers was done at two different levels of the Str, namely the rostral Str, closer to the site of transplant, and the caudal Str, further from the site of transplant. In the rostral Str, there was a 66% decrease in TH+fiber density in buffer-transplanted mice compared to control animals ( $P < 0.0001$  for IL and  $P = 0.0002$  for CL), which was alleviated by hNSC transplant as the TH+area increased by 55% ( $P = 0.0026$  for IL and  $P = 0.0056$  for CL) (Fig. 1b). The same pattern occurred in the caudal Str, with a decrease of approximately 47% in TH+fiber density in buffer-treated mice compared to controls ( $P = 0.0001$  for IL and  $P = 0.0002$  for CL), while mice transplanted with hVM1 clone 32 cells had an increased TH+area of around 43% compared to buffer-treated animals ( $P = 0.0002$  for IL and  $P = 0.0002$  for CL) (Fig. 1c). In the SNpc, there was a 74% decrease in the TH+immunoreactivity in buffer-treated mice compared to control animals ( $P < 0.0001$  for IL and  $P = 0.0002$  for CL), and hNSC-treated mice showed a recuperation of 58% in TH+area in the SNpc compared to buffer-treated mice ( $P = 0.0159$  for IL and  $P = 0.0211$  for CL). Controls had more nigral TH expression than hNSC-treated mice, with an increase of 43% on the IL side and 29% on the CL side; this reached significance only on the IL side ( $P = 0.0063$ ) (Fig. 1d). Thus, it can be stated that the transplant of hVM1 clone 32 cells significantly prevented the damage to the nigrostriatal pathway in MPTP-treated mice four months post-transplant.

When comparing TH expression in the rostral Str between one and four months post-transplant (Fig. 1a left vs. Figure 1b), there was a 20% and 23% increase in the TH+area percentages in the buffer-treated and hNSC-transplanted groups, respectively. In the SNpc, there was a marginal difference (less than 1%) in the TH+area percentages of each MPTP-treated experimental group at one and four months post-transplant (Fig. 1a right vs. Figure 1d). Therefore, this indicates that there was negligible spontaneous dopaminergic sprouting in the rostral Str and none in the SNpc, and that hNSC transplantation maintained nigrostriatal TH expression between one and four months post-transplant.

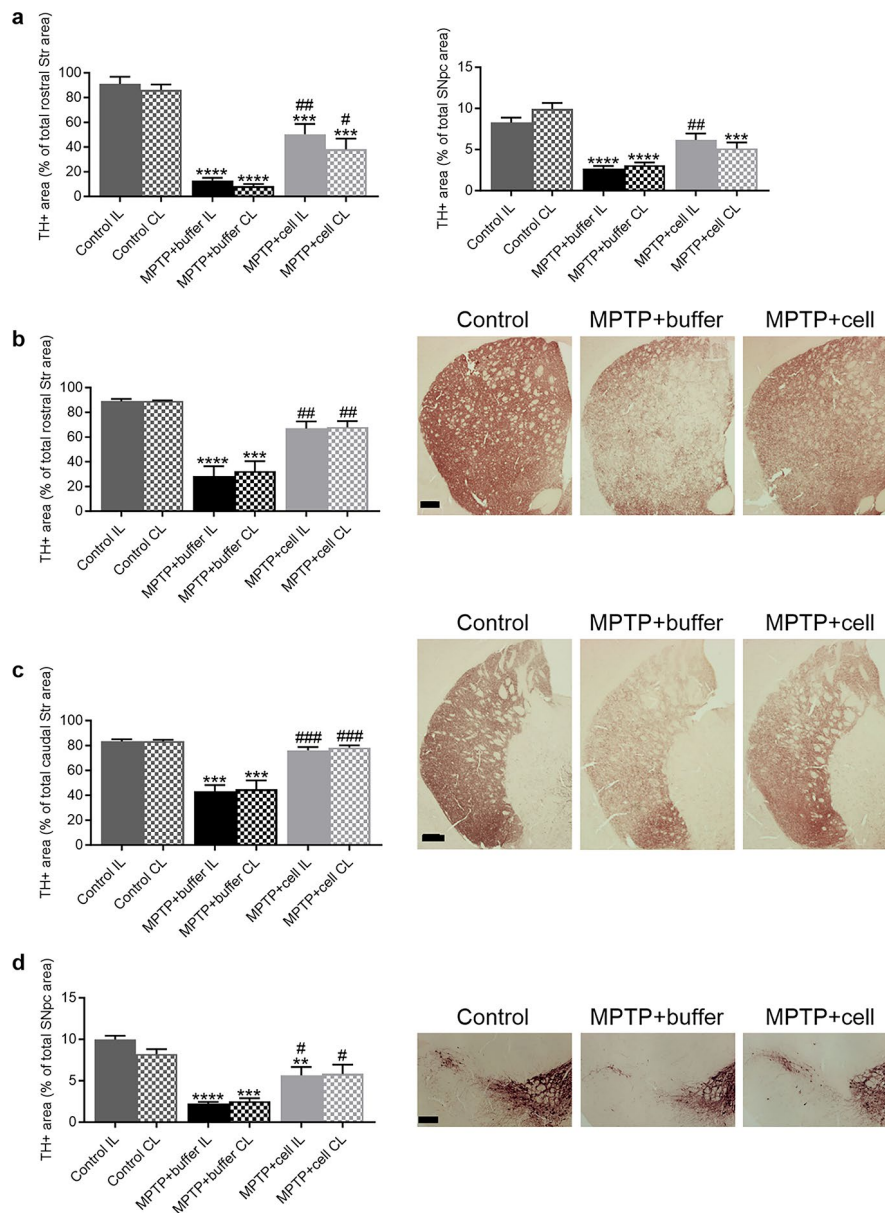


**Fig. 1** Nigrostriatal pathway degeneration and protection. **a left** One month post-transplant, striatal TH+ fibers were decreased in buffer-treated mice compared to controls (\*\*\*\* $P < 0.0001$  for IL and \*\*\*\*  $P < 0.0001$  for CL). Transplantation of hNSCs alleviated this decrease (## $P = 0.0019$  for IL and # $P = 0.0176$  for CL). Controls had more TH expression than hNSC-treated animals (\*\*\* $P = 0.0009$  for IL and \*\*\* $P = 0.0004$  for CL). Control  $n = 5$ , MPTP + buffer  $n = 6$ , MPTP + cell  $n = 7$ . **a right** One month post-transplant, TH+ area was decreased in the SNpc in buffer-treated animals compared to control mice (\*\*\*\* $P < 0.0001$  for IL and \*\*\*\* $P < 0.0001$  for CL). Cell-transplanted animals had increased nigral TH immunoreactivity compared to those that received buffer, reaching significance on the IL side (## $P = 0.0063$ ). Control mice had increased TH expression compared to hNSC-transplanted animals; this was significant on only the CL side (\*\*\* $P = 0.0002$ ). Control  $n = 6$ , MPTP + buffer  $n = 5$ , MPTP + cell  $n = 5$ . **b** Four months post-transplant, in the rostral Str, TH+ area decreased in buffer-treated animals compared to controls (\*\*\*\* $P < 0.0001$  for IL and \*\*\* $P = 0.0002$  for CL) while TH expression was increased in hNSC-transplanted mice compared to those that received buffer (## $P = 0.0026$  for IL and ## $P = 0.0056$  for CL). Control  $n = 3$ , MPTP + buffer  $n = 5$ , MPTP + cell  $n = 5$ . **c** Likewise, caudal striatal TH immunostaining declined in buffer-transplanted animals compared to control mice (\*\*\* $P = 0.0001$  for IL and \*\*\* $P = 0.0002$  for CL), and was recovered in hNSC-treated animals (### $P = 0.0002$  for IL and ### $P = 0.0002$  for CL). Control  $n = 3$ , MPTP + buffer  $n = 5$ , MPTP + cell  $n = 5$ . **d** In the SNpc, TH+ area % was lower in buffer-treated mice compared to control animals (\*\*\*\* $P < 0.0001$  for IL and \*\*\* $P = 0.0002$  for CL). Mice transplanted with hNSCs had increased nigral TH expression compared to animals treated with buffer (# $P = 0.0159$  for IL and # $P = 0.0211$  for CL). Control animals had more TH immunostaining in the SNpc compared to hNSC-treated mice, but this was statistically significant on only the IL side (\*\* $P = 0.0063$ ). Control  $n = 3$ , MPTP + buffer  $n = 5$ , MPTP + cell  $n = 4$ . **a-d** One-way ANOVA followed by Tukey's post-hoc test. \* = compared to same brain hemisphere of Control, # = compared to same brain hemisphere of MPTP + buffer. Scale bars **b-d** = 200  $\mu\text{m}$ . IL = ipsilateral, CL = contralateral, hNSC = human neural stem cell, Str = striatum, SNpc = substantia nigra pars compacta

### Activity and gait alterations

Several behavioral aspects were measured to examine the effects of MPTP and hNSC transplant four months post-transplant. In the OFT, there were no significant differences among the three experimental groups in terms of distance travelled, time spent grooming, time spent rearing, urination, and defecation (data not shown). In addition, buffer-treated mice spent almost 51% more time in the center compared to controls, indicating hyperactivity ( $P=0.0383$ ). Although not statistically significant, this increased time spent in the center had a tendency to decrease by 35% in hNSC-treated mice (Fig. 2a). The PPT was employed to study differences in gait between the three groups of animals. Stride length tended to be an average of 10% shorter in all MPTP-treated animals, only

attaining statistical significance in the case of the forelimb of those transplanted with hNSCs ( $P=0.0373$  for CL and  $P=0.0207$  for IL) (Fig. 2b). All MPTP-treated mice tended to have a shorter forelimb stride width of approximately 10% compared to controls, but this was only statistically significant on the IL-CL side ( $P=0.0415$  for MPTP+buffer vs. Control and  $P=0.0195$  for MPTP+cell vs. Control). Hindlimb stride width was similar in all three experimental groups (Fig. 2c).

### Inflammatory reaction in the nigrostriatal pathway and lymph nodes

The inflammatory reaction in the brain was studied in the two main regions of interest, namely the rostral Str and SNpc, in order to see if there were differences in

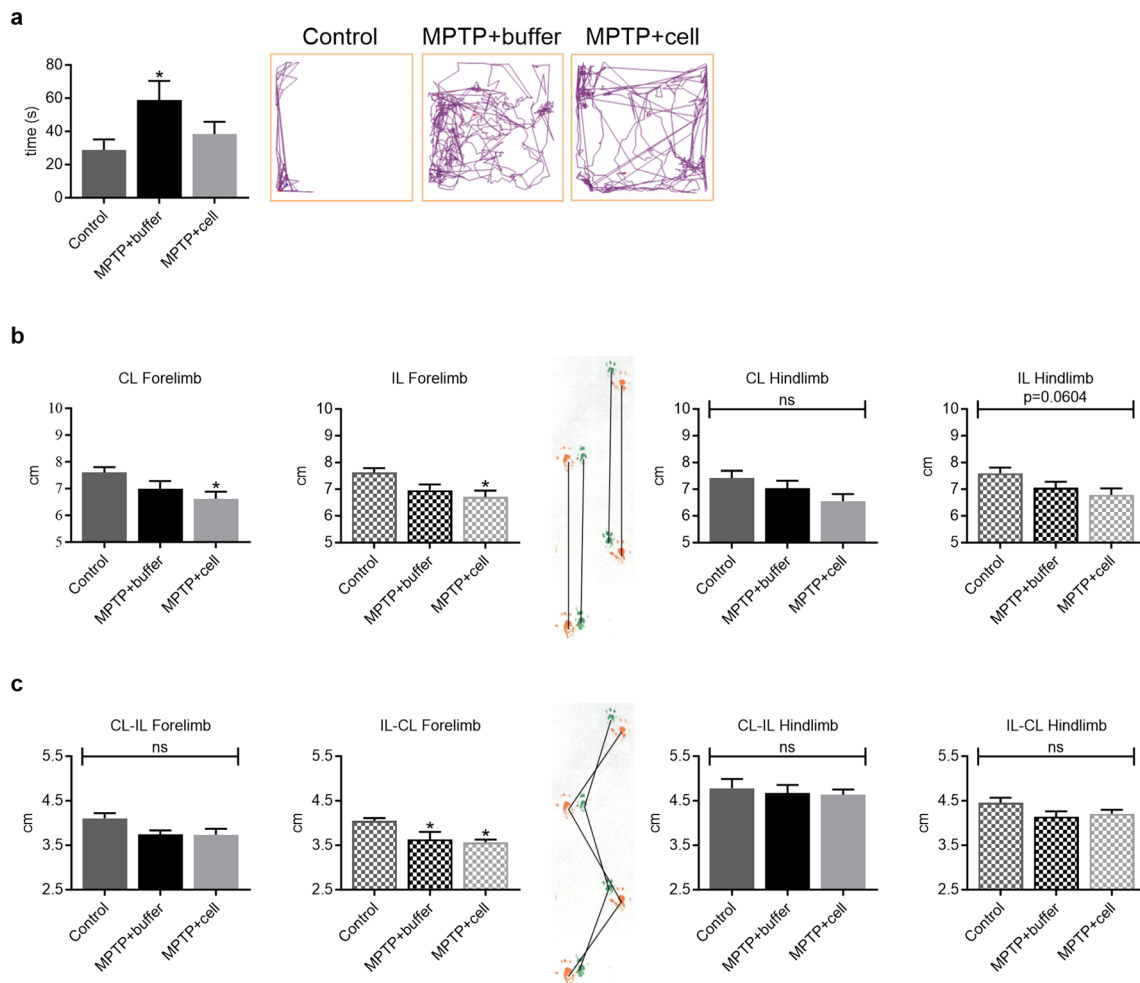


**Fig. 2** Behavioral studies demonstrated changes in activity and gait. **a** Four months post-transplant, buffer-treated mice spent more time in the center of the OFT box compared to controls ( $*P=0.0383$ ), while hNSC-transplanted mice tended to spend less time in the center compared to those that received buffer. Control  $n=15$ , MPTP + buffer  $n=12$ , MPTP + cell  $n=13$ . **b** Forelimb and hindlimb stride length tended to decrease in all MPTP-treated mice compared to control animals; this reached statistical significance only in the case of the forelimbs of hNSC-transplanted mice ( $*P=0.0373$  for CL and  $*P=0.0207$  for IL). Control  $n=6$ , MPTP + buffer  $n=4$ , MPTP + cell  $n=4$ . **c** Forelimb stride width tended to be shorter in mice intoxicated with MPTP, attaining statistical significance on one side ( $*P=0.0415$  for MPTP + buffer vs. Control and  $*P=0.0195$  for MPTP + cell vs. Control), while hindlimb stride width was unchanged among the three experimental groups. Control  $n=6$ , MPTP + buffer  $n=4$ , MPTP + cell  $n=4$ . **a-c** One-way ANOVA followed by Tukey’s post-hoc test. \* = compared to Control, ns = not significant. IL = ipsilateral, CL = contralateral, hNSC = human neural stem cell, OFT = open field test



glial populations between the experimental groups four months post-transplant. In the rostral Str, control and buffer-treated animals had a similar amount of GFAP immunostaining, marking astrocytes. The rostral Str IL to the side of the transplant in animals grafted with hVM1 clone 32 cells had a larger GFAP+ area compared to control ( $P < 0.0001$ ) and buffer-treated ( $P < 0.0001$ ) mice, and had almost twice as much astroglial immunoreactivity than the rostral Str CL to the side of transplant of hNSC-treated animals ( $P = 0.0088$ ). Moreover, the rostral Str CL to the side of the transplant of hNSC-treated mice tended to have two-four times more GFAP immunostaining than control and buffer-transplanted animals, which reached statistical significance when compared to the CL rostral Str of these two experimental groups ( $P = 0.0102$  vs. MPTP+buffer and  $P = 0.0170$  vs. Control) (Fig. 3a). In the SNpc, GFAP+ area was similar across all experimental groups (data not shown). Inflammation was further studied in the SNpc, by marking microglia via Iba1 immunostaining. There was a clear trend in that all MPTP-treated mice showed an average of almost four times more nigral Iba1 immunoreactivity compared to controls, attaining statistical significance in the case of the IL side in buffer-treated animals ( $P = 0.0345$ ) and the CL side in cell-transplanted mice ( $P = 0.0123$ ). Morphological analysis revealed the Iba1+ microglia in the SNpc of all experimental groups to have small and round cell bodies with ramifications, which is typical of resting microglia (Fig. 3b).

Data on inflammation in the central nervous system (CNS) showed that there was a distinct pattern of astroglial and microglial activation in hNSC-treated mice. In addition to this, immunosuppression with CSA inhibits the adaptive immune response [40], thus allowing to see what happens to the innate immune system. Therefore, it was decided that the focus would be MCs, innate immune cells located in the CNS and LNs, recently shown to be connected to the CNS [41–44]. Four months post-transplant, analysis of the superficial cervical LNs showed a trend in that all MPTP-treated mice had larger LNs compared to control animals ( $P = 0.0561$ ) (Fig. 4a). Moreover, MC density quantification revealed that hNSC-transplanted mice displayed a tendency of increased MC density compared to both buffer-treated and control animals, which was statistically significant when controls and hNSC-transplanted mice were compared ( $P = 0.0127$ ). Stem cell-treated animals had almost double the MC density compared to buffer-treated mice which in turn had more than twice the MC density of that of controls (Fig. 4b). In the CNS, there was no quantifiable amount of MCs in either the Str or SNpc (data not shown).

### Changes in neurogenesis in the SVZ and SGZ

Neurogenesis was studied in the SVZ and SGZ in order to explore the notion of how the transplant affected each stage of neurogenesis four months post-transplant. Immunostaining was done for NES and Ki-67, neural stem cell (NSC) markers, and DCX, a marker for immature neurons. In the SVZ, there were no differences in the amount of NES immunostaining nor the number of Ki-67+ cells between the three experimental groups (Fig. 5a). By contrast, there was a strong tendency for all MPTP-treated mice to have 22–44% less DCX expression compared to controls, reaching statistical significance when the CL SVZ of control mice was compared to both SVZs of buffer-treated ( $P = 0.0126$  for IL and  $P = 0.0203$  for CL) and the IL SVZ of cell-transplanted ( $P = 0.0197$ ) animals (Fig. 5b).

In the SGZ, there was either no expression or no quantifiable amount of either NES or Ki-67. These immunostainings were done using a 10 week-old naïve mouse brain as a control, which clearly marked NES+ and Ki-67+ NSCs in this hippocampal region. Another marker for NSCs, GFAP, showed similar expression in all three experimental groups (data not shown). Neuroblasts exhibited a completely different pattern in this hippocampal region. Control animals showed variation in DCX expression in the SGZ, and there was a tendency for DCX immunostaining to decrease by approximately 71% in buffer-treated animals, although only statistically significant when comparing the CL SGZ of buffer-transplanted mice to the IL SGZ of controls ( $P = 0.0402$ ). Transplantation with hVM1 clone 32 cells alleviated this decline as hNSC-transplanted mice showed increased DCX+ area, which attained statistical significance when compared to the CL SGZ of buffer-treated animals ( $P = 0.0427$  for IL and  $P = 0.0468$  for CL). Moreover, there were no differences in DCX expression between the control and hNSC-grafted groups (Fig. 6a). Additionally, Iba1+ populations, which had small and round soma across all experimental groups, tended to decrease in the SGZ by almost 50% in hNSC-transplanted animals compared to control and buffer-treated mice. This reached statistical significance when the IL SGZ of cell-treated and control mice were compared ( $P = 0.0282$ ) (Fig. 6b). It is interesting to note that the most significant improvements upon transplantation were the restoration of TH+ fibers and cells in the Str and SNpc, respectively, and the rescue of immature neurons in the SGZ. Therefore, the Pearson correlation coefficient ( $r$ ) between these groups was calculated. The  $r$  value correlating TH+ area percentage in the rostral and caudal Str, with DCX+ area percentage in the SGZ was 0.935 ( $P < 0.0001$ ) (Fig. 6c left), and the correlation coefficient correlating TH+ area percentage in the SNpc with DCX+ area percentage in the SGZ was 0.891 ( $P = 0.0173$ ) (Fig. 6c right). Although the correlation was stronger

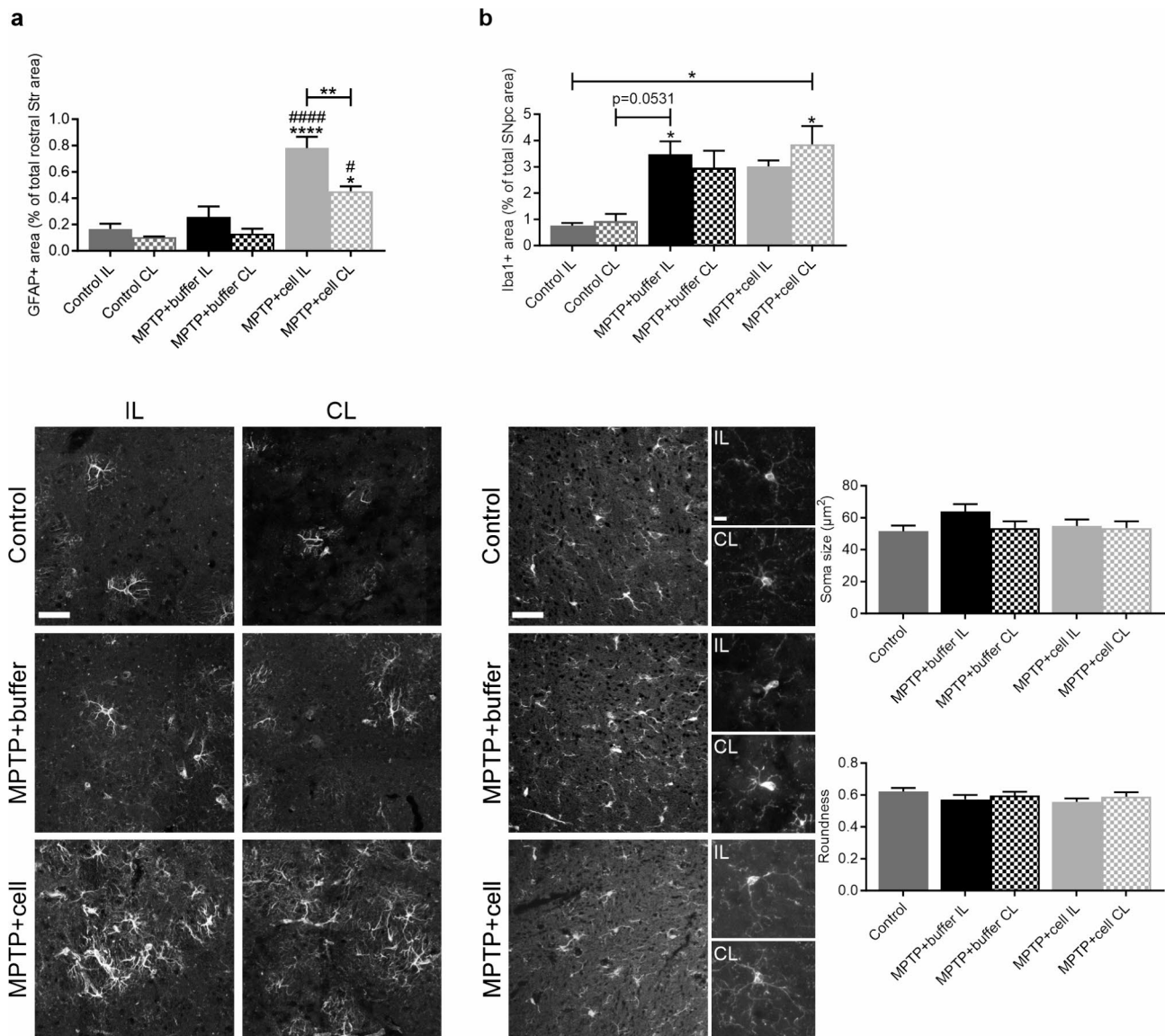


**Fig. 3** Inflammatory reaction of astrocytes and microglia in the nigrostriatal pathway. **a** Four months post-transplant, rostral striatal GFAP+ area was similar in control and buffer-treated animals, and tended to be higher on the CL side to the transplant in hNSC-transplanted mice, although this was only statistically significant when compared to the CL rostral Str of buffer-treated ( $\#P=0.0102$ ) and control ( $*P=0.0170$ ) animals. Expression of GFAP in the IL rostral Str in hNSC-treated mice was increased compared to the rostral Str of all control ( $****P<0.0001$ ) and buffer-treated ( $#####P<0.0001$ ) animals, and to a lesser extent compared to the CL rostral Str of those that received cells ( $**P=0.0088$ ). Control  $n=3$ , MPTP+buffer  $n=5$ , MPTP+cell  $n=5$ . **b** In the SNpc, Iba1 expression tended to be higher in all MPTP-treated mice compared to controls, reaching statistical significance in the case of the IL rostral Str of those treated with buffer ( $*P=0.0345$  vs. Control IL) and the CL rostral Str of hNSC-transplanted animals ( $*P=0.0123$  vs. Control IL and  $*P=0.0194$  vs. Control CL). These Iba1+ microglia were small, round and ramified, and soma size and roundness were not altered across all experimental groups. Control  $n=3$ , MPTP+buffer  $n=5$ , MPTP+cell  $n=5$ . **a, b** One-way ANOVA followed by Tukey’s post-hoc test. \* = compared to same brain hemisphere of Control, # = compared to same brain hemisphere of MPTP+buffer. Scale bar **a**=50 µm and scale bars **b**=50 µm (left images) and 10 µm (right zoom images). IL=ipsilateral, CL=contralateral, hNSC=human neural stem cell, Str=striatum, SNpc=substantia nigra pars compacta

between DCX expression in the SGZ to TH expression in the Str rather than the SNpc, both correlation coefficients were very high and emphasize the important relationship between the nigrostriatal pathway and hippocampal neurogenesis.

**Survival, differentiation, and maturation, of engrafted cells**

A few surviving hVM1 clone 32 hNSCs were detected in the Str of some, but not all, animals, four months post-grafting (Fig. 7). Some cells were found at the transplantation site (Fig. 7a, b) whereas others were located in other parts of the Str (Fig. 7c, d). No hNSCs were detected in the SNpc or hippocampus (Hip) of transplanted animals.

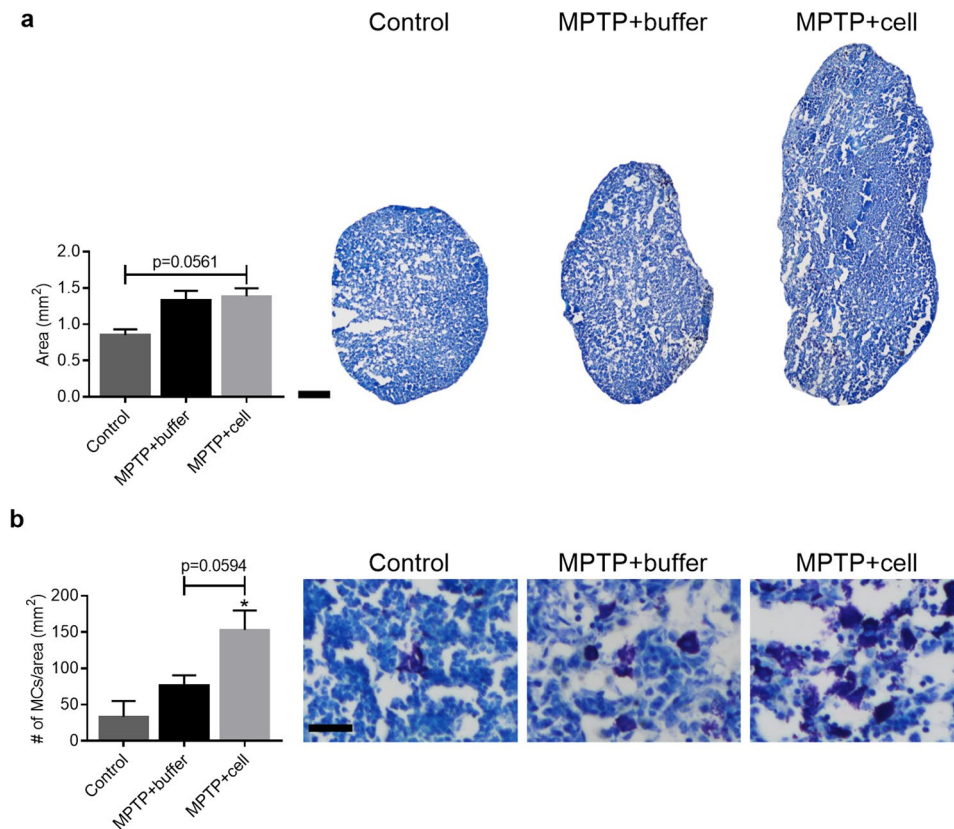


**Fig. 4** Characterization of superficial cervical LN size and MC density. **a** Four months post-transplant, animals intoxicated with MPTP tended to have larger LNs compared to control mice ( $P=0.0561$ ). Control  $n=3$ , MPTP +buffer  $n=7$ , MPTP +cell  $n=9$ . **b** Mast cell density in the LNs tended to be increased in hNSC-transplanted animals, but only in a statistically significant manner when compared to controls ( $*P=0.0127$ ). Control  $n=3$ , MPTP +buffer  $n=5$ , MPTP +cell  $n=5$ . \* = compared to Control. **a, b** One-way ANOVA followed by Tukey's post-hoc test. Scale bar **a**=200  $\mu\text{m}$  and scale bar **b**=25  $\mu\text{m}$ . LN=lymph node, MC=mast cell, hNSC=human neural stem cell

Therefore, this indicates that there was little to no graft survival. Although transplanted cells did not label for GFAP, they were in close contact with the host's astrocytes (Fig. 7e-g).

#### Cell-secreted factors in vitro and their expression in vivo

Because the transplanted cells did not survive, how the cells succeeded in exerting beneficial effects such as nigrostriatal pathway recovery and increased hippocampal neurogenesis remained unexplained. The literature says that cell survival is low in experimental PD and clinical trials, but human cells are usually found. In this case they were not, and because it has been elucidated that most cells die within the first week of transplantation [26, 45, 46], hVM1 clone 32 cells were differentiated in vitro for seven days and the CM was collected. The CM of the hNSCs in proliferation and differentiation conditions were analyzed to see if the cells were secreting any factors that may be beneficial to Parkinsonian mice upon transplantation. There was no GDNF detected in either basal proliferation medium (20/20+) or proliferation CM, and increased in a non-significant manner in differentiation CM compared to the latter. This NTF is a

difficult analyte to study under differentiation conditions because although basal levels of differentiation media (Lotharius) components are subtracted from CM levels, GDNF is added to the media during the medium change several times throughout the hNSC differentiation protocol. Furthermore, concentrations of BDNF, FKN, SCE, VEGF-A, and VEGF-C, were all increased in differentiation compared to proliferation CM ( $P=0.0002$  for BDNF,  $P<0.0001$  for FKN,  $P=0.0092$  for SCE,  $P=0.0355$  for VEGF-A, and  $P=0.0002$  for VEGF-C) (Fig. 8a).

To make the connection between in vitro and in vivo results, striatal expression of two factors, BDNF and FKN, were measured via immunofluorescence four months post-transplant. These two factors were chosen because they had the lowest (BDNF) and highest (FKN) concentrations, and the most significant difference in concentration between proliferation and differentiation conditions in vitro. As well, out of all the other factors analyzed, BDNF and FKN have the highest expression in the mouse Str in vivo. The antibodies used recognized both human and mouse proteins. In the rostral Str, the BDNF+area had a tendency to increase by 51% in hNSC-transplanted mice compared to animals treated with

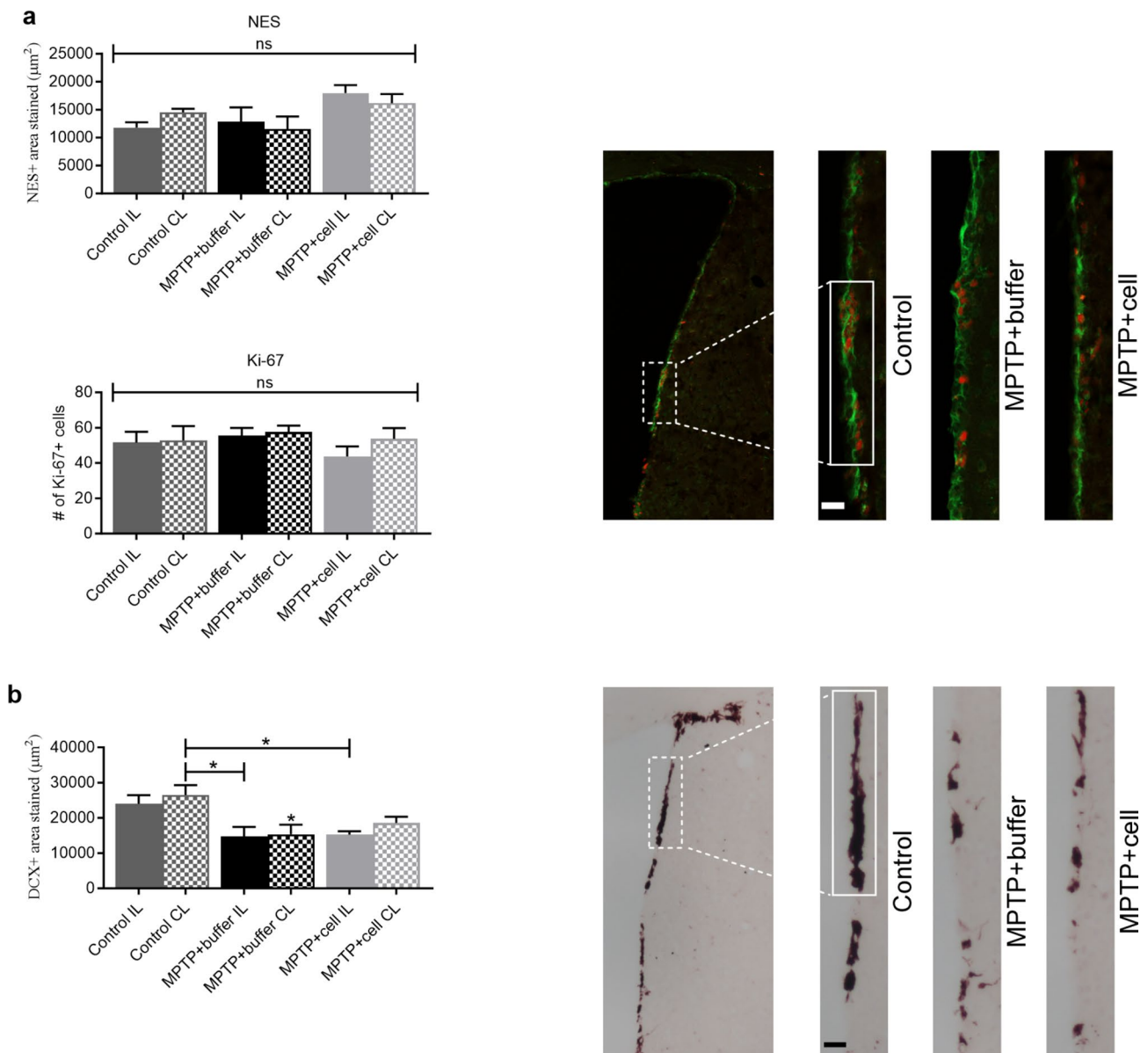


**Fig. 5** Changes in NSC and neuroblast populations in the SVZ. **a** Four months post-transplant, NES+ area stained (green; top) and the number of Ki-67+ cells (red; bottom), were similar across all experimental groups. Control  $n=3$ , MPTP + buffer  $n=5$ , MPTP + cell  $n=5$ . ns = not significant. **b** Expression of DCX tended to decrease in all MPTP-treated mice compared to controls; this decline was statistically significant when the CL SVZ of the control group was compared to both SVZs of buffer-treated ( $*P=0.0126$  for IL and  $*P=0.0203$  for CL) and the IL SVZ of cell-transplanted ( $*P=0.0197$ ) animals. Control  $n=7$ , MPTP + buffer  $n=9$ , MPTP + cell  $n=9$ . \* = compared to same brain hemisphere of Control. **a, b** One-way ANOVA followed by Tukey’s post-hoc test. Scale bars = 25 µm. IL = ipsilateral, CL = contralateral, NSC = neural stem cell, SVZ = subventricular zone

buffer (Fig. 8b). Meanwhile, FKN expression in the rostral Str was similar in all control and MPTP-intoxicated mice (Fig. 8c).

**Discussion**

Our data show that four months post-transplant, hNSC-transplanted animals exhibited a recovery of TH+ fibers at both levels of the Str studied, and of TH+ cells in the SNpc, with the former being more considerable. One month post-transplant, TH expression was also increased

in the rostral Str and SNpc. In addition, we were able to see that the MPTP experimental model was working and that minimal spontaneous dopaminergic sprouting occurred in the rostral Str, but not in the SNpc. This spontaneous recovery in the Str has been shown to occur between ten days to five months post-MPTP administration depending on the publication. However, these studies were done in mice between the ages of eight and ten weeks when the compensatory mechanisms are still fully functioning, and spontaneous dopaminergic sprouting

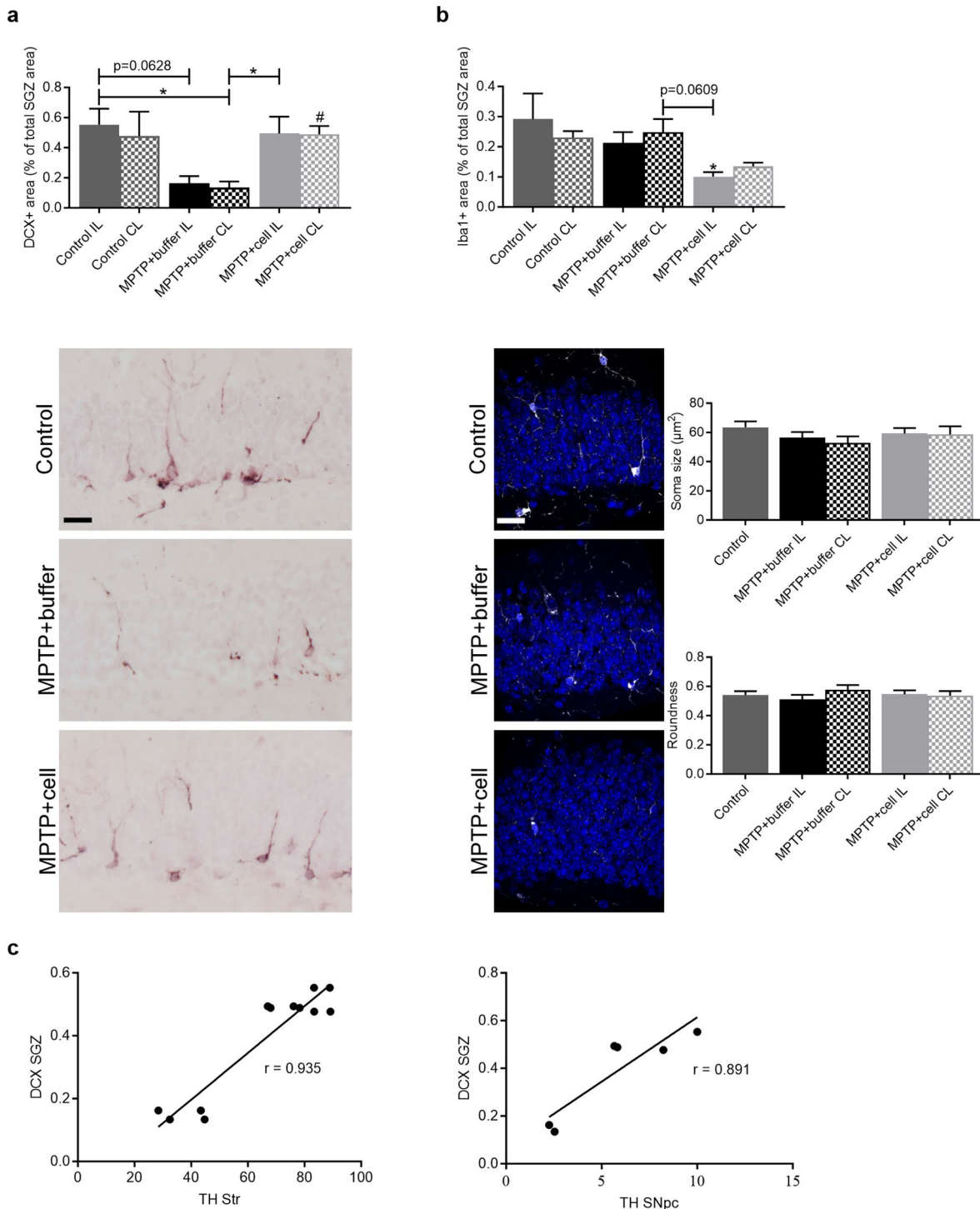


**Fig. 6** Increased neurogenesis and reduced inflammation in the SGZ. **a** Four months post-transplant, controls had varying expression levels of DCX in the SGZ while buffer-treated animals tended to have lower expression, which reached statistical significance when the CL SGZ of buffer-transplanted and the IL SGZ of control mice were compared ( $*P=0.0402$ ). DCX+ area % was increased in hNSC-transplanted mice compared to those that received buffer; this attained statistical significance when compared to the CL SGZ of buffer-treated animals ( $*P=0.0427$  for IL and  $\#P=0.0468$  for CL). Control  $n=3$ , MPTP + buffer  $n=5$ , MPTP + cell  $n=5$ . **b** In the SGZ, mice transplanted with hNSCs tended to have lower Iba1 + area compared to both control and buffer-treated animals, although only statistically significant when the IL SGZ of cell-treated and control mice were compared ( $*P=0.0282$ ). These Iba1 + microglia had small and round soma in all animals. Control  $n=3$ , MPTP + buffer  $n=5$ , MPTP + cell  $n=5$ . **a, b** One-way ANOVA followed by Tukey’s post-hoc test. \* = compared to same brain hemisphere of Control, # = compared to same brain hemisphere of MPTP + buffer. Scale bar **a** = 50 µm and scale bar **b** = 25 µm. **c** The correlation between DCX expression in the SGZ and TH expression in the Str (**left**) and SNpc (**right**) was 0.935 ( $P<0.0001$ ) and 0.891 ( $P=0.0173$ ), respectively. Pearson correlation coefficient ( $r$ ); Number of Str XY pairs = 12, Number of SNpc XY pairs = 6. IL = ipsilateral, CL = contralateral, hNSC = human neural stem cell, SGZ = subgranular zone, Str = striatum, SNpc = substantia nigra pars compacta

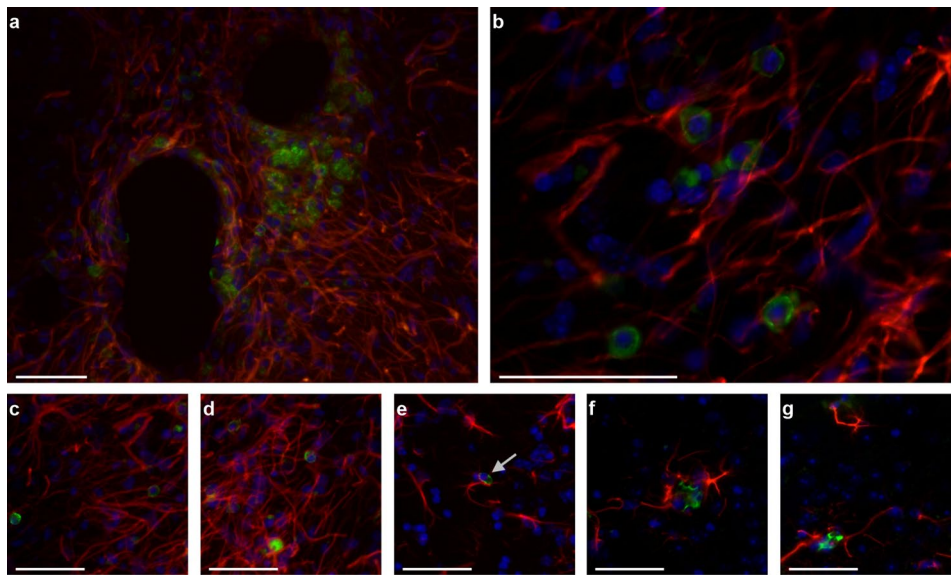


**Fig. 7** Survival, differentiation, and maturation, of transplanted hVM1 clone 32 cells. Transplanted cells were stained with STEM121 (green), which marks human-specific cytoplasm. Mouse and human astrocytes were marked with GFAP (red), and nuclei with DAPI (blue). **a** Surviving transplanted hNSCs and astrocytes at the transplantation site in the Str four months post-transplant. **b** Zoom image of **a**. **c, d** Transplanted hNSCs and astrocytes in other parts of the Str. **e-g** Close-up images of transplanted cells with arrow in **e** indicating apoptotic-like nucleus. Scale bars **a, c-g**=50  $\mu\text{m}$  and scale bar **b**=100  $\mu\text{m}$ . hNSC=human neural stem cell, Str=striatum

was not observed in older (eight month-old) mice. Furthermore, although some studies found no spontaneous dopaminergic recovery in the SNpc in either the younger or older MPTP-treated mice [47–50] as is the case of this study, there are two reports of spontaneous nigral dopaminergic neurogenesis in mice treated with MPTP [51, 52]. Therefore, although some spontaneous dopaminergic sprouting did occur in the rostral Str, it occurred practically equally in both buffer- and cell-treated mice and therefore this does not take away from the fact that the transplantation of hNSCs provides striatal dopaminergic neuroprotection as shown by TH expression.

In this study, hyperactivity, as measured by time spent in the center in the OFT, was observed in MPTP-treated mice, and tended to be improved with hNSC transplant. Furthermore, parameters measuring anxiety were not affected by MPTP treatment or hNSC transplant. Depletion of DA in the prefrontal cortex has been shown to increase hyperactivity and decrease anxiety, and this hyperactivity is due to disinhibition and attention deficit [53]. Hyperactivity could be explained by increased norepinephrine (NE) levels in the Str [54]. Furthermore, attention deficit and impulsivity occur in some PD patients [55–57].

With one parameter changed among the exploratory and anxiety behaviors, and gait marginally affected, our findings reveal that nigrostriatal TH expression levels did not coincide with behavioral changes. The neurotoxin MPTP shows varying behavioral effects in mice, with solid, consistent, long-lasting deficits yet to be shown [53,

54, 58–60]. Other publications have also demonstrated that MPTP-treated mice can show behavioral recovery or no difference in behavior compared to controls from four days to two months post-injection while maintaining a significantly damaged nigrostriatal system [52, 54, 61, 62]. Additionally, alterations in NE levels and DA metabolite ratios were possibly responsible for the disconnect between the nigrostriatal pathway and behavioral symptoms. It has been reported that NE plays a compensatory role in MPTP-treated mouse behavior, but its levels vary depending on the report. In one study, NE levels increased after striatal DA depletion, and there were no behavioral deficits [54], while in another, NE depletion in Str in a MPTP model led to no changes in distance moved or number of rears, and less grooming [63]. Likewise, damage to the NE system occurs in PD patients [54]. A more defined compensatory mechanism that occurs in experimental PD models as well as in PD patients is the increase in DA metabolite ratios 3,4-Dihydroxyphenylacetic acid/DA and Homovanillic acid/DA in the Str, which indicate DA turnover. This compensation leads to a lack of behavioral deficits [53, 54, 63].

Although using MPTP to model PD led to minimal spontaneous dopaminergic sprouting in the rostral Str, and unsynchronized nigrostriatal TH expression and behavioral symptoms, MPTP still remains one of the best models available to mimic human PD pathology [64]. Another way to induce PD is chronic MPTP treatment; however, this is complicated due to the intrinsic difficulty of working with MPTP, a neurotoxin harmful

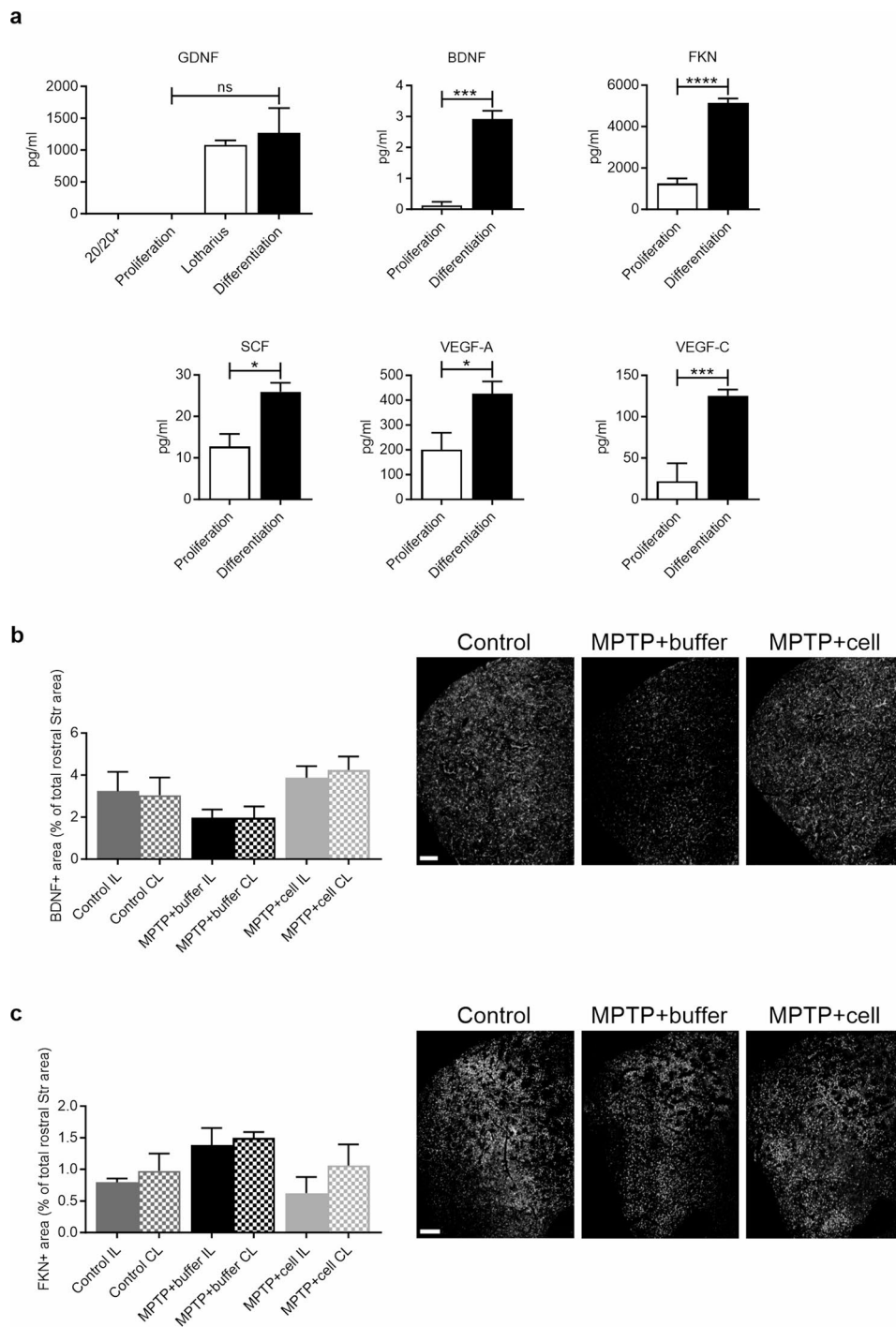


**Fig. 8** Factors secreted by cells in vitro and striatal expression of BDNF and FKN in vivo. **a** While GDNF levels only tended to rise, concentrations (pg/ml) of BDNF, FKN, SCF, VEGF-A, and VEGF-C, were all increased in differentiation compared to proliferation CM (GDNF  $P=0.0750$ ; BDNF  $****P=0.0002$ ; FKN  $****P<0.0001$ ; SCF  $**P=0.0092$ ; VEGF-A  $*P=0.0355$ ; VEGF-C  $***P=0.0002$ ). Two-tailed unpaired t-tests. 20/20+  $n=2$ , Lotharius  $n=2$ , Proliferation CM  $n=3$ , Differentiation CM  $n=8$  except for GDNF where  $n=7$ . ns = not significant. **b** Four months post-transplant, in the rostral Str, hNSC-transplanted mice tended to have increased BDNF immunostaining compared to those which received buffer. Control  $n=3$ , MPTP + buffer  $n=3$ , MPTP + cell  $n=4$ . Scale bar = 200  $\mu$ m. **c** Striatal FKN expression was similar across all experimental groups four months post-transplant. Control  $n=3$ , MPTP + buffer  $n=4$ , MPTP + cell  $n=4$ . **b, c** One-way ANOVA followed by Tukey's post-hoc test. Scale bars = 200  $\mu$ m. CM = conditioned media, hNSC = human neural stem cell, Str = striatum

to humans as well. Moreover, the administration of 6-hydroxydopamine (6-OHDA) remains safer but does not provide whole-body DA degeneration. Pre-clinical studies like this one done in rodents are needed to test hNSC transplantation [38, 65]. In the present study, the best approach was using this MPTP protocol, but like any other, it had its pitfalls. More importantly though, differences were observed between both MPTP-treated groups in several key aspects involved in PD pathology thus allowing for the differentiation of the outcome with and without cell therapy.

Astrocytes and microglia play a pivotal role in neuroinflammation, a main feature of PD, although it remains to be understood whether the CNS inflammatory response is the cause or effect of PD [66]. Our results show that hNSC transplant increased astroglial populations in the rostral Str and that MPTP intoxication led to increased microglial presence in the SNpc, showing the distinct reaction of these two inflammatory molecules. It has been reported that when the acute MPTP protocol was implemented in male mice, astroglial and microglial populations in Str were the same as in controls but these glial populations were increased in SNpc compared to controls, more than two months post-MPTP treatment [61]. Other experimental CRT studies found no changes in GFAP expression in the Str or SNpc among cell-treated and vehicle-treated Parkinsonian animals [67, 68], which is in contrast to the findings presented.

In this study, MPTP-treated mice tended to have larger LNs compared to controls four months post-transplant. This peripheral inflammation has not been vastly explored in PD, but it was found that alpha-synuclein drains from the CNS to the LNs in MPTP-treated mice [69] and deep cervical LNs significantly increase in size in an A53T-overexpressing transgenic mouse model [70]. Mice transplanted with hNSCs tended to have increased MC density in the superficial cervical LNs compared to the other experimental groups. This demonstrates that the transplant had an influence on non-CNS structures and processes, re-emphasizing the connection between the CNS and LNs [39–42]. As well, it shows that MCs are affected by hNSC transplantation, although, per our results, MCs did not appear to be contributing to inflammation in the CNS as they were practically not present. Mast cell populations have not been analyzed before in CRT studies within the PD field. However, MC migration has been shown to be required for immunosuppression [71] and it has been demonstrated both *in vitro* and *in vivo* that MCs, activated by glia maturation factor, release factors that promote neurodegeneration, neuroinflammation, and behavioral deficits, in PD [72, 73].

Inflammation is known to play a capricious role in PD and other chronic neurodegenerative disorders like Alzheimer's disease. While increased neurogenesis can

be triggered by a brain insult, exacerbated microglial activation is linked to impaired basal and insult-induced hippocampal neurogenesis [74]. Our data in the SVZ indicate that NES and Ki-67 expression showed no change while DCX+ area was decreased upon MPTP intoxication in the SVZ. In one publication, 6-OHDA-lesioned adult female mice were transplanted with hNSCs, and SVZ changes were analyzed; the transplant restored DA receptor D1, DA transporter, NeuN, and TH, in the SVZ, which had decreased expression upon 6-OHDA lesion. Expression of Ki-67 was unchanged in control, buffer-treated, and cell-treated groups, consistent with our findings. Although SVZ neurogenesis was partially rescued and there were behavioral improvements in hNSC-transplanted mice, striatal TH expression was recovered over time in 6-OHDA-lesioned mice and the significant decrease in TH+ cells in the SN was not alleviated by transplant [68]. In another study using 6-OHDA-lesioned rats, hNSCs induced behavioral and nigrostriatal TH expression recovery along with increased neurogenesis as shown via DCX immunostaining in the SVZ compared to buffer-treated animals [21]. It is also important to consider that increased SVZ neurogenesis has been observed in several PD models where damage to the nigrostriatal pathway on its own generates this increase in neural progenitor cells so this may also affect neurogenesis result interpretation [75–77].

In the SGZ, we found practically no NES+ or Ki-67+ NSC populations, and GFAP expression was similar in all experimental groups. At the time of sacrifice, the animals used in this study were nine months old, an age when neurogenesis has been shown to be decreased in the neurogenic niches, especially the SGZ. Therefore, it is not surprising that some proliferating cell populations were shown to be practically null in the SGZ because although it has been shown that hippocampal neurogenesis is not completely eradicated in older rodents, monkeys, and even humans, it is indeed drastically reduced [78–81].

The neuroblast population, as shown by DCX immunostaining, decreased in buffer-treated animals and was alleviated by hVM1 clone 32 cell transplant. Hence, the transplant was capable of restoring hippocampal neurogenesis, suggesting that local recovery mechanisms were set in motion. In addition, we found a high correlation between TH expression in the Str and SNpc, and DCX expression in the SGZ, thus supporting the reported connection between DA and hippocampal neurogenesis [82, 83]. Although it has been described that neuroinflammation depletes neurogenesis, increased levels of astrocytes in the rostral Str and increased levels of microglia in the SNpc did not negatively affect neurogenesis in this study [74, 85–87]. Our analysis of hippocampal inflammation demonstrates that microglial populations had a



tendency to decrease in hNSC-treated mice, suggesting that lower microglia reaction could have contributed to increased neurogenesis. While the increase in microglia in the SNpc of MPTP-treated animals and the decrease in microglia in the SGZ of hNSC-transplanted mice may seem contradictory, it has been shown that microglia have differential phenotypes, reactivity, and expression levels depending on the brain region [88–90]. In Doorn et al., similar to the present study, Iba1+microglia were increased in the SNpc of PD patients compared to controls, but these microglia had the same level of expression in the Hip of both groups. Nonetheless, in both the SNpc and Hip, controls had more ramified microglia with a small rounded cell body, associated with so-called “resting”, surveying microglia, while PD patients had more microglia with few or no ramifications and an amoeboid cell body, which is typical of reactive or activated microglia [88]. In another publication, the amount of Iba1+microglia was unchanged in the SNpc, Hip, and prefrontal cortex, among control and PD patients, except for the amygdala which showed increased microglial populations in PD patients. However, besides the SNpc, the regions were quantified by counting human leukocyte antigen DR immunoreactive amoeboid-shaped microglia only [89]. The protein Iba1 is expressed in all microglia and is therefore a general marker for all microglia, both resting and reactive [90, 91]. From our morphological analysis, Iba1+microglia in the SNpc and SGZ were small, round and ramified, indicating that they are in a surveying, resting state [37].

Interestingly, the IL and CL sides were affected equally in all three experimental groups which is reflected in the behavioral results as paw print patterns are the same for both sides. There was one exception: expression of GFAP in hNSC-transplanted mice, where the IL rostral Str had almost twice as much GFAP+area than its CL equivalent. The astrocytes did not react to the MPTP, but only to the hNSC transplant, most notably at the exact transplantation site. Although the mice were administered CSA, there was a clear augmentation of astrocytes in response to the cell transplant, which could explain cell death.

Although future experiments are needed to include and compare samples from control mice one week post-MPTP treatment and control mice given sham surgery, these groups were not included in this study in order to decrease the number of animals used and increase overall feasibility of the animal experiments, and because our main interest was to compare Parkinsonian mice receiving cell and vehicle transplant.

Various experimental CRT studies in Parkinsonian rodents using hNSCs of fetal brain origin have shown TH expression recovery in the Str and SNpc, while fewer have explored or found behavioral improvement and SVZ neurogenesis increase, compared to buffer-treated

animals. Moreover, several publications have reported graft survival months after transplant, which did not occur in this report [21, 67].

Since we found an irrelevant number of surviving transplanted cells in the Str, the majority of them must have either migrated or died. However, there were also no hVM1 clone 32 cells in other brain regions such as the SNpc and Hip. Therefore, although the initial goal was to see if the transplanted hVM1 clone 32 cells could replace and take over the functions of the lost or impaired DAN to improve symptoms in adult Parkinsonian mice, since the transplanted cells died, these hNSCs in this specific model actually generated neuroprotection rather than cell replacement.

Cell survival is a persistent problem in CRT; even in the most successful clinical trials in PD patients to date, there is low graft survival. Around 95% of transplanted cells die in experimental PD animals and PD patients shortly after transplantation [26, 45, 46]. In this particular study, nor the CSA dose nor the CSA injection protocol was the cause of transplanted cell death because the equivalent protocol was used in Parkinsonian rats, and the cells survived two months post-grafting [29]. Several articles have demonstrated that cells transplanted in the brain of rodents can survive even without immunosuppression, although to a much lesser extent than in animals receiving CSA, and that graft survival is identical in experiments implementing non-daily injections of CSA or removal of CSA immunosuppression after three weeks compared to those using more severe or longer immunosuppression protocols, respectively [39, 65, 92]. Moreover, hVM1 clone 32 cell survival was negligible four months post-transplant in middle-aged Parkinsonian mice [30]. When comparing graft survival in mouse and rat, the time of transplantation could be very important because in Ramos-Moreno et al., rats were transplanted five weeks after 6-OHDA lesion [29] while mice in this study were transplanted one week after MPTP lesion. This four-week difference could be critical in terms of DAN death, pro-inflammatory cytokine release, mitochondrial dysfunction, apoptosis, and autophagy processes occurring after neurotoxin injection, which after five weeks are probably more stabilized than after one week. In addition, there is evidence of very low or complete lack of cell survival of CNS transplants in mice compared to rats [65].

Stem cells can act directly or indirectly by either integrating into the brain or by releasing factors like NTFs, thus leading to improvement upon transplantation [93]. Therefore, the more plausible explanation in this study is that the transplanted cells died, and that before dying, these cells released factors BDNF, FKN, GDNF, SCF, VEGF-A, and VEGF-C, leading to the beneficial effects of increased nigrostriatal TH immunostaining

and hippocampal neurogenesis in hNSC-transplanted mice. Because the factors were more abundant in the Str, the transplantation site, than the SNpc, the nigrostriatal pathway recovery was better in the Str. All of the aforementioned NTFs have all been shown to protect DAN in control conditions and experimental PD models in vitro and in vivo [13–22, 94]. Specifically, in MPTP-treated monkeys, BDNF infusion prevented SNpc DAN loss [95]. Also, physical exercise is beneficial in PD patients at all stages of the disease, providing control of motor symptoms and an improved quality of life; the basis of this improvement is that physical exercise increases BDNF levels in PD animals and patients [96]. In one study, expression of TH in the Str and SNpc, and motor symptoms, were exacerbated when BDNF receptors were blocked in the Str of 6-OHDA-lesioned rats [97]. Furthermore, continuous intrastriatal infusion of FKN in Parkinsonian rats led to rescued TH expression and decreased microglial activation in the Str and SNpc [16], and treatment with soluble FKN improved motor deficits, increased TH+expression in Str, and rescued NeuN+ and TH+ cell populations in the SNpc of MPTP-treated mice [14]. The NTFs BDNF, GDNF, and VEGF, promote neurogenesis [85, 86, 98], while FKN represses microglia [14, 16, 99]. Neurotrophic factors, CM, and the encapsulation of cells that are genetically modified to secrete GDNF, have been shown to be beneficial in experimental PD models, thus strengthening the argument for the influence of cell-secreted factors [22, 28, 100–102]. In this study, rostral striatal FKN expression was similar in all experimental groups. However, BDNF immunostaining differences were observed in the rostral Str, with hNSC-transplanted mice tending to have more BDNF expression compared to buffer-treated animals, thus paralleling the same pattern observed in striatal and nigral TH expression. This suggests that the BDNF secreted by the hVM1 clone 32 cells aided in the beneficial effects observed in hNSC-transplanted mice. In addition to the BDNF secreted by the hNSCs, a greater number of astrocytes in the rostral Str of cell-transplanted mice may have contributed to elevated striatal BDNF levels as astrocytes produce and secrete BDNF [103, 104]. Moreover, there is a positive feedback loop involving BDNF in that when BDNF interacts with its receptor TrkB, BDNF expression is increased [105, 106]. Therefore, it is possible that the BDNF released from the transplanted hNSCs generated a continuous increase in BDNF which in turn led to the neuroprotective effects seen in the cell-transplanted Parkinsonian mice.

Age is a determining factor in the outcome of CRT in both animal models of PD and human PD patients. It has been shown that CRT has more clinically beneficial outcomes in younger patients with less advanced PD [26, 28]. When middle-aged Parkinsonian mice were

transplanted with hVM1 clone 32 cells, there was minimal restoration of dopaminergic cell populations in the Str and SNpc [30], while in adult Parkinsonian mice treated with these hNSCs, the nigrostriatal pathway was protected. The response of adult and middle-aged brains to CRT is different, with the younger CNS more capable of activating recovery mechanisms as we see in the present study. The distinct results of CRT in adult and middle-aged mice shows the importance of taking into consideration the age of recipient when choosing candidates for CRT as a treatment and when assessing clinical trial results. Although there are limitations on the use of hVM1 clone 32 cells due to their fetal origin, *v-myc* immortalization and lack of survival in experimental PD mice, which renders them unusable in clinical trials, these hNSCs support the fact that CRT is a plausible and effective treatment for PD.

## Conclusions

In summary, there has yet to be a more complete report of the effects of hNSCs derived from fetal brain. In this comprehensive study, the transplantation of hVM1 clone 32 cells in a bilateral PD mouse model led to the rescue of nigrostriatal TH+populations and the restoration of hippocampal neurogenesis in adult Parkinsonian mice through a neuroprotective effect plausibly involving the factors secreted by the hVM1 clone 32 cells. Further research is warranted, but these results support the long-lasting beneficial effects of hNSC transplantation for the treatment of PD.

## Abbreviations

|        |  |
|--------|--|
| 6-OHDA | 6-hydroxydopamine                            |
| ANOVA  | Analysis of variance                         |
| BDNF   | Brain-derived neurotrophic factor            |
| CL     | Contralateral                                |
| CM     | Conditioned media                            |
| CNS    | Central nervous system                       |
| CRT    | Cell replacement therapy                     |
| CSA    | Cyclosporine A                               |
| DCX    | Doublecortin                                 |
| DA     | Dopamine                                     |
| DAN    | Dopaminergic neurons                         |
| FKN    | Fractalkine                                  |
| GDNF   | Glial cell-derived neurotrophic factor       |
| GFAP   | Glial fibrillary acidic protein              |
| Hip    | Hippocampus                                  |
| hNSC   | Human neural stem cell                       |
| Iba1   | Ionized calcium-binding adapter molecule 1   |
| IL     | Ipsilateral                                  |
| LN     | Lymph node                                   |
| MC     | Mast cell                                    |
| MPTP   | 1-methyl-4-phenyl-1,2,3,6-tetrahydropyridine |
| NE     | Norepinephrine                               |
| NES    | Nestin                                       |
| NSC    | Neural stem cell                             |
| NTF    | Neurotrophic factor                          |
| OFT    | Open field test                              |
| PD     | Parkinson's disease                          |
| PPT    | Paw print test                               |
| SCF    | Stem cell factor                             |
| SGZ    | Subgranular zone                             |

|        |                                      |
|--------|--------------------------------------|
| SNpc   | Substantia nigra pars compacta       |
| Str    | Striatum                             |
| SVZ    | Subventricular zone                  |
| TH     | Tyrosine hydroxylase                 |
| VEGF-A | Vascular endothelial growth factor A |
| VEGF-C | Vascular endothelial growth factor C |

### Acknowledgements

The authors would like to give a special thank you to Alberto Martínez-Serrano for his many years of leadership and guidance in the laboratory. The authors also thank the Animal Facility and the Advanced Light Microscopy Facility at the Centro de Biología Molecular Severo Ochoa for their help and support.

### Author contributions

AN and MPP conceived and designed the study. AN, SGL, and MPP acquired the data. AN and MPP analyzed and interpreted the data. AN drafted the manuscript. AN, JRC, and MPP substantively revised and edited the manuscript. JRC and MPP supervised all aspects of the study. MPP obtained study funding. All authors read and approved the final manuscript.

### Funding

This work was funded by the Spanish Cell Therapy Network-Instituto de Salud Carlos III (TerCel ISCIII) (RETICS RD16/0011/0032), the Spanish Ministry of Economy and Competitiveness (SAF 2014-56101-R), and the Spanish Ministry of Science and Innovation (PID2020-118189RB-I00). The funding bodies were not involved in the design of the study, collection, analysis, and interpretation of data, or writing of the manuscript.

### Data availability

The datasets used and analysed during the current study are available from the corresponding authors on reasonable request.

### Declarations

#### Ethics approval and consent to participate

All animal work and use of hNSCs were approved by the Universidad Autónoma de Madrid (CEI 62-1077-A079; 06/03/2015) and the Comunidad de Madrid (PROEX149/15; 29/05/2015) Research Ethics Committees, both with project title "Desarrollo hacia la clínica del trasplante de células troncales neurales humanas para la enfermedad de Parkinson".

#### Consent for publication

Not applicable.

#### Competing interests

The authors declare that they have no competing interests.

#### Artificial intelligence

The authors declare that artificial intelligence is not used in this study.

Received: 23 February 2024 / Accepted: 30 September 2024

Published online: 09 October 2024

### References

- De Virgilio A, Greco A, Fabbrini G, Inghilleri M, Rizzo MI, Gallo A, et al. Parkinson's disease: autoimmunity and neuroinflammation. *Autoimmun Rev*. 2016;15(10):1005–11.
- Kalia LV, Lang AE. Parkinson's disease. *Lancet*. 2015;386(9996):896–912.
- Lesage S, Brice A. Parkinson's disease: from monogenic forms to genetic susceptibility factors. *Hum Mol Genet*. 2009;18(R1):R48–59.
- Wirdefeldt K, Adami HO, Cole P, Trichopoulos D, Mandel J. Epidemiology and etiology of Parkinson's disease: a review of the evidence. *Eur J Epidemiol*. 2011;26(Suppl 1):S1–58.
- Allen SJ, Watson JJ, Shoemark DK, Barua NU, Patel NK. GDNF, NGF and BDNF as therapeutic options for neurodegeneration. *Pharmacol Ther*. 2013;138(2):155–75.
- Chauhan NB, Siegel GJ, Lee JM. Depletion of glial cell line-derived neurotrophic factor in substantia nigra neurons of Parkinson's disease brain. *J Chem Neuroanat*. 2001;21(4):277–88.
- Sarkar S, Raymick J, Imam S. Neuroprotective and Therapeutic Strategies against Parkinson's Disease: Recent Perspectives. *Int J Mol Sci*. 2016;17(6). <https://doi.org/10.3390/ijms17060904>.
- Akerud P, Holm PC, Castelo-Branco G, Sousa K, Rodriguez FJ, Arenas E. Persephin-overexpressing neural stem cells regulate the function of nigral dopaminergic neurons and prevent their degeneration in a model of Parkinson's disease. *Mol Cell Neurosci*. 2002;21(2):205–22.
- Sampaio TB, Savall AS, Gutierrez MEZ, Pinton S. Neurotrophic factors in Alzheimer's and Parkinson's diseases: implications for pathogenesis and therapy. *Neural Regen Res*. 2017;12(4):549–57.
- Sullivan AM, Toulouse A. Neurotrophic factors for the treatment of Parkinson's disease. *Cytokine Growth Factor Rev*. 2011;22(3):157–65.
- Tome D, Fonseca CP, Campos FL, Baltazar G. Role of neurotrophic factors in Parkinson's Disease. *Curr Pharm Des*. 2017;23(5):809–38.
- Xiao N, Le QT. Neurotrophic factors and their potential applications in tissue regeneration. *Arch Immunol Ther Exp (Warsz)*. 2016;64(2):89–99.
- Caballero B, Sherman SJ, Falk T. Insights into the mechanisms involved in Protective effects of VEGF-B in dopaminergic neurons. *Parkinsons Dis*. 2017;2017:4263795.
- Morganti JM, Nash KR, Grimmig BA, Ranjit S, Small B, Bickford PC, et al. The soluble isoform of CX3CL1 is necessary for neuroprotection in a mouse model of Parkinson's disease. *J Neurosci*. 2012;32(42):14592–601.
- Nash KR, Moran P, Finneran DJ, Hudson C, Robinson J, Morgan D, et al. Fractalkine over expression suppresses alpha-synuclein-mediated neurodegeneration. *Mol Ther*. 2015;23(1):17–23.
- Pabon MM, Bachstetter AD, Hudson CE, Gemma C, Bickford PC. CX3CL1 reduces neurotoxicity and microglial activation in a rat model of Parkinson's disease. *J Neuroinflammation*. 2011;8:9. -2094-8-9.
- Piltonen M, Planken A, Leskela O, Myohanen TT, Hanninen AL, Auvinen P, et al. Vascular endothelial growth factor C acts as a neurotrophic factor for dopamine neurons in vitro and in vivo. *Neuroscience*. 2011;192:550–63.
- Tian YY, Tang CJ, Wang JN, Feng Y, Chen XW, Wang L, et al. Favorable effects of VEGF gene transfer on a rat model of Parkinson disease using adeno-associated viral vectors. *Neurosci Lett*. 2007;421(3):239–44.
- Yasuhara T, Shingo T, Kobayashi K, Takeuchi A, Yano A, Muraoka K, et al. Neuroprotective effects of vascular endothelial growth factor (VEGF) upon dopaminergic neurons in a rat model of Parkinson's disease. *Eur J Neurosci*. 2004;19(6):1494–504.
- Yasuhara T, Shingo T, Muraoka K, Kameda M, Agari T, Wen Ji Y, et al. Neurorescue effects of VEGF on a rat model of Parkinson's disease. *Brain Res*. 2005;1053(1–2):10–8.
- Yasuhara T, Matsukawa N, Hara K, Yu G, Xu L, Maki M, et al. Transplantation of human neural stem cells exerts neuroprotection in a rat model of Parkinson's disease. *J Neurosci*. 2006;26(48):12497–511.
- Yasuhara T, Date I. Intracerebral transplantation of genetically engineered cells for Parkinson's disease: toward clinical application. *Cell Transpl*. 2007;16(2):125–32.
- Stoker TB, Torsney KM, Barker RA. Emerging treatment approaches for Parkinson's Disease. *Front Neurosci*. 2018;12:693.
- Hallett PJ, Cooper O, Sadi D, Robertson H, Mendez I, Isacson O. Long-term health of dopaminergic neuron transplants in Parkinson's disease patients. *Cell Rep*. 2014;7(6):1755–61.
- Li W, Englund E, Widner H, Mattsson B, van Westen D, Latt J, et al. Extensive graft-derived dopaminergic innervation is maintained 24 years after transplantation in the degenerating parkinsonian brain. *Proc Natl Acad Sci U S A*. 2016;113(23):6544–9.
- Stoker TB, Barker RA. Cell therapies for Parkinson's disease: how far have we come? *Regen Med*. 2016;11(8):777–86.
- U.S. National Library of Medicine. <https://clinicaltrials.gov>. (2023). Accessed 1 April 2023.
- Yasuhara T, Kameda M, Sasaki T, Tajiri N, Date I. Cell therapy for Parkinson's Disease. *Cell Transpl*. 2017;26(9):1551–9.
- Ramos-Moreno T, Lendinez JG, Pino-Barrio MJ, Del Arco A, Martínez-Serrano A. Clonal human fetal ventral mesencephalic dopaminergic neuron precursors for cell therapy research. *PLoS ONE*. 2012;7(12):e52714.
- Nelke A, García-López S, Martínez-Serrano A, Pereira MP. Multifactoriality of Parkinson's disease as explored through human neural stem cells and their transplantation in Middle-aged parkinsonian mice. *Front Pharmacol*. 2022;12:773925.
- Villa A, Liste I, Courtois ET, Seiz EG, Ramos M, Meyer M, et al. Generation and properties of a new human ventral mesencephalic neural stem cell line. *Exp Cell Res*. 2009;315(11):1860–74.

32. Lotharius J, Barg S, Wiekop P, Lundberg C, Raymon HK, Brundin P. Effect of mutant alpha-synuclein on dopamine homeostasis in a new human mesencephalic cell line. *J Biol Chem*. 2002;277(41):38884–94.
33. Jackson-Lewis V, Przedborski S. Protocol for the MPTP mouse model of Parkinson's disease. *Nat Protoc*. 2007;2(1):141–51.
34. Formentini L, Pereira MP, Sanchez-Cenizo L, Santacatterina F, Lucas JJ, Navarro C, et al. In vivo inhibition of the mitochondrial H<sup>+</sup>-ATP synthase in neurons promotes metabolic preconditioning. *EMBO J*. 2014;33(7):762–78.
35. Prut L, Belzung C. The open field as a paradigm to measure the effects of drugs on anxiety-like behaviors: a review. *Eur J Pharmacol*. 2003;463(1–3):3–33.
36. Paxinos G, Franklin KBJ. The mouse brain in stereotaxic coordinates. 2nd ed. San Diego: Academic; 2001.
37. Davis BM, Salinas-Navarro M, Cordeiro MF, Moons L, De Groef L. Characterizing microglia activation: a spatial statistics approach to maximize information extraction. *Sci Rep*. 2017;7(1):1576.
38. Heuer A, Kirkeby A, Pfisterer U, Jönsson ME, Parmar M. hESC-derived neural progenitors prevent xenograft rejection through neonatal desensitisation. *Exp Neurol*. 2016;282:78–85.
39. Villadiego J, Romo-Madero S, García-Swinburn R, Suárez-Luna N, Bermejo-Navas A, Echevarría M, et al. Long-term immunosuppression for CNS mouse xenotransplantation: effects on nigrostriatal neurodegeneration and neuroprotective carotid body cell therapy. *Xenotransplantation*. 2018;25(6):e12410.
40. Matsuda S, Koyasu S. Mechanisms of action of cyclosporine. *Immunopharmacology*. 2000;47(2–3):119–25.
41. Aspelund A, Antila S, Proulx ST, Karlén TV, Karaman S, Detmar M, et al. A dural lymphatic vascular system that drains brain interstitial fluid and macromolecules. *J Exp Med*. 2015;212(7):991–9.
42. Huang J, Zhu C, Zhang P, Zhu Q, Liu Y, Zhu Z, et al. S100+ cells: a new neuro-immune cross-talkers in lymph organs. *Sci Rep*. 2013;3:1114.
43. Louveau A, Smirnov I, Keyes TJ, Eccles JD, Rouhani SJ, Peske JD, et al. Structural and functional features of central nervous system lymphatic vessels. *Nature*. 2015;523(7560):337–41.
44. Wulff C, Gunther HS. Dendritic cells and macrophages neurally hard-wired in the lymph node. *Sci Rep*. 2015;5:16866.
45. Emgard M, Hallin U, Karlsson J, Bahr BA, Brundin P, Blomgren K. Both apoptosis and necrosis occur early after intracerebral grafting of ventral mesencephalic tissue: a role for protease activation. *J Neurochem*. 2003;86(5):1223–32.
46. Rafuse VF, Soundararajan P, Leopold C, Robertson HA. Neuroprotective properties of cultured neural progenitor cells are associated with the production of sonic hedgehog. *Neuroscience*. 2005;131(4):899–916.
47. Bezdard E, Dovero S, Imbert C, Boraud T, Gross CE. Spontaneous long-term compensatory dopaminergic sprouting in MPTP-treated mice. *Synapse*. 2000;38(3):363–8.
48. Ho A, Blum M. Induction of interleukin-1 associated with compensatory dopaminergic sprouting in the denervated striatum of young mice: model of aging and neurodegenerative disease. *J Neurosci*. 1998;18(15):5614–29.
49. Jakowec MW, Nixon K, Hogg E, McNeill T, Petzinger GM. Tyrosine hydroxylase and dopamine transporter expression following 1-methyl-4-phenyl-1,2,3,6-tetrahydropyridine-induced neurodegeneration of the mouse nigrostriatal pathway. *J Neurosci Res*. 2004;76(4):539–50.
50. Mitsumoto Y, Watanabe A, Mori A, Koga N. Spontaneous regeneration of nigrostriatal dopaminergic neurons in MPTP-treated C57BL/6 mice. *Biochem Biophys Res Commun*. 1998;248(3):660–3.
51. Shan X, Chi L, Bishop M, Luo C, Lien L, Zhang Z, Liu R. Enhanced de novo neurogenesis and dopaminergic neurogenesis in the substantia nigra of 1-methyl-4-phenyl-1,2,3,6-tetrahydropyridine-induced Parkinson's disease-like mice. *Stem Cells*. 2006;24(5):1280–7.
52. Zhao M, Momma S, Delfani K, Carlén M, Cassidy RM, Johansson CB, et al. Evidence for neurogenesis in the adult mammalian substantia nigra. *Proc Natl Acad Sci U S A*. 2003;100(13):7925–30.
53. Rousselet E, Joubert C, Callebert J, Parain K, Tremblay L, Orioux G, et al. Behavioral changes are not directly related to striatal monoamine levels, number of nigral neurons, or dose of parkinsonian toxin MPTP in mice. *Neurobiol Dis*. 2003;14(2):218–28.
54. Zhang QS, Heng Y, Mou Z, Huang JY, Yuan YH, Chen NH. Reassessment of subacute MPTP-treated mice as animal model of Parkinson's disease. *Acta Pharmacol Sin*. 2017;38(10):1317–28.
55. Kehagia AA, Housden CR, Regenthal R, Barker RA, Muller U, Rowe J, et al. Targeting impulsivity in Parkinson's disease using atomoxetine. *Brain*. 2014;137(Pt 7):1986–97.
56. Nieoullon A. Dopamine and the regulation of cognition and attention. *Prog Neurobiol*. 2002;67(1):53–83.
57. Nombela C, Rittman T, Robbins TW, Rowe JB. Multiple modes of impulsivity in Parkinson's disease. *PLoS ONE*. 2014;9(1):e85747.
58. Blandini F, Armentero MT. Animal models of Parkinson's disease. *FEBS J*. 2012;279(7):1156–66.
59. Blesa J, Przedborski S. Parkinson's disease: animal models and dopaminergic cell vulnerability. *Front Neuroanat*. 2014;8:155.
60. Meredith GE, Rademacher DJ. MPTP mouse models of Parkinson's disease: an update. *J Parkinsons Dis*. 2011;1(1):19–33.
61. Huang D, Wang Z, Tong J, Wang M, Wang J, Xu J, et al. Long-term changes in the Nigrostriatal Pathway in the MPTP Mouse Model of Parkinson's Disease. *Neuroscience*. 2018;369:303–13.
62. Schwarting RK, Sedelis M, Hofe K, Auburger GW, Huston JP. Strain-dependent recovery of open-field behavior and striatal dopamine deficiency in the mouse MPTP model of Parkinson's disease. *Neurotox Res*. 1999;1(1):41–56.
63. Luchtman DW, Shao D, Song C. Behavior, neurotransmitters and inflammation in three regimens of the MPTP mouse model of Parkinson's disease. *Physiol Behav*. 2009;98(1–2):130–8.
64. Przedborski S, Jackson-Lewis V, Naini AB, Jakowec M, Petzinger G, Miller R, et al. The parkinsonian toxin 1-methyl-4-phenyl-1,2,3,6-tetrahydropyridine (MPTP): a technical review of its utility and safety. *J Neurochem*. 2001;76(5):1265–74.
65. Robertson VH, Evans AE, Harrison DJ, Precious SV, Dunnett SB, Kelly CM, et al. Is the adult mouse striatum a hostile host for neural transplant survival? *Neuroreport*. 2013;24(18):1010–1015.
66. Troncoso-Escudero P, Parra A, Nassif M, Vidal RL. Outside in: unraveling the role of Neuroinflammation in the progression of Parkinson's Disease. *Front Neurol*. 2018;9:860.
67. Zuo FX, Bao XJ, Sun XC, Wu J, Bai QR, Chen G, et al. Transplantation of human neural stem cells in a Parkinsonian Model exerts Neuroprotection via Regulation of the Host Microenvironment. *Int J Mol Sci*. 2015;16(11):26473–92.
68. Zuo F, Xiong F, Wang X, Li X, Wang R, Ge W, et al. Intrastriatal transplantation of human neural stem cells restores the impaired Subventricular Zone in Parkinsonian mice. *Stem Cells*. 2017;35(6):1519–31.
69. Benner EJ, Banerjee R, Reynolds AD, Sherman S, Pisarev VM, Tshiperson V, et al. Nitrated alpha-synuclein immunity accelerates degeneration of nigral dopaminergic neurons. *PLoS ONE*. 2008;3(1):e1376.
70. Liu Z, Huang Y, Wang X, Li JY, Zhang C, Yang Y, et al. The cervical lymph node contributes to peripheral inflammation related to Parkinson's disease. *J Neuroinflammation*. 2023;20(1):93.
71. da Silva EZ, Jamur MC, Oliver C. Mast cell function: a new vision of an old cell. *J Histochem Cytochem*. 2014;62(10):698–738.
72. Kempuraj D, Selvakumar GP, Zaheer S, Thangavel R, Ahmed ME, Raikwar S, et al. Cross-talk between Glia, neurons and Mast Cells in Neuroinflammation Associated with Parkinson's Disease. *J Neuroimmune Pharmacol*. 2018;13(1):100–12.
73. Selvakumar GP, Ahmed ME, Thangavel R, Kempuraj D, Dubova I, Raikwar SP, et al. A role for glia maturation factor dependent activation of mast cells and microglia in MPTP induced dopamine loss and behavioural deficits in mice. *Brain Behav Immun*. 2020;87:429–43.
74. Ekdahl CT, Claassen JH, Bonde S, Kokaia Z, Lindvall O. Inflammation is detrimental for neurogenesis in adult brain. *Proc Natl Acad Sci U S A*. 2003;100(23):13632–7.
75. Aponso PM, Faull RLM, Connor B. Increased progenitor cell proliferation and astrogenesis in the partial progressive 6-hydroxydopamine model of Parkinson's disease. *Neuroscience*. 2008;151(4):1142–53.
76. Mourtz T, Dimitrakopoulos D, Kakogiannis D, Salodimitris C, Botsakis K, Meri DK, et al. Characterization of substantia nigra neurogenesis in homeostasis and dopaminergic degeneration: beneficial effects of the microneurotrophin BNN-20. *Stem Cell Res Ther*. 2021;12(1):335.
77. Xie MQ, Chen ZC, Zhang P, Huang HJ, Wang TT, Ding YQ, et al. Newborn dopaminergic neurons are associated with the migration and differentiation of SVZ-derived neural progenitors in a 6-hydroxydopamine-injected mouse model. *Neuroscience*. 2017;352:64–78.
78. Ben Abdallah NM, Slomianka L, Vysotski AL, Lipp HP. Early age-related changes in adult hippocampal neurogenesis in C57 mice. *Neurobiol Aging*. 2010;31(1):151–61.
79. Jabès A, Lavenex PB, Amaral DG, Lavenex P. Quantitative analysis of postnatal neurogenesis and neuron number in the macaque monkey dentate gyrus. *Eur J Neurosci*. 2010;31(2):273–85.

80. Jin K, Sun Y, Xie L, Bateau S, Mao XO, Smelick C, et al. Neurogenesis and aging: FGF-2 and HB-EGF restore neurogenesis in hippocampus and subventricular zone of aged mice. *Aging Cell*. 2003;2(3):175–83.
81. Kuhn HG, Dickinson-Anson H, Gage FH. Neurogenesis in the dentate gyrus of the adult rat: age-related decrease of neuronal progenitor proliferation. *J Neurosci*. 1996;16(6):2027–33.
82. Takamura N, Nakagawa S, Masuda T, Boku S, Kato A, Song N et al. The effect of dopamine on adult hippocampal neurogenesis. *Prog Neuropsychopharmacol Biol Psychiatry*. 2014;50:116–24.
83. Zhang T, Hong J, Di T, Chen L. MPTP impairs dopamine D1 receptor-mediated survival of newborn neurons in ventral Hippocampus to cause depressive-like behaviors in adult mice. *Front Mol Neurosci*. 2016;9:101.
84. Pluchino S, Muzio L, Imitola J, Deleidi M, Alfaro-Cervello C, Salani G, et al. Persistent inflammation alters the function of the endogenous brain stem cell compartment. *Brain*. 2008;131(Pt 10):2564–78.
85. Shohayeb B, Diab M, Ahmed M, Ng DCH. Factors that influence adult neurogenesis as potential therapy. *Transl Neurodegener*. 2018;7:4–018. eCollection 2018.
86. Yang P, Arnold SA, Habas A, Hetman M, Hagg T. Ciliary neurotrophic factor mediates dopamine D2 receptor-induced CNS neurogenesis in adult mice. *J Neurosci*. 2008;28(9):2231–41.
87. Doorn KJ, Lucassen PJ, Boddeke HW, Prins M, Berendse HW, Drukarch B, et al. Emerging roles of microglial activation and non-motor symptoms in Parkinson's disease. *Prog Neurobiol*. 2012;98(2):222–38.
88. Doorn KJ, Moors T, Drukarch B, van de Berg WD, Lucassen PJ, van Dam AM. Microglial phenotypes and toll-like receptor 2 in the substantia nigra and hippocampus of incidental Lewy body disease cases and Parkinson's disease patients. *Acta Neuropathol Commun*. 2014;2:90–014.
89. Kouli A, Camacho M, Allinson K, Williams-Gray CH. Neuroinflammation and protein pathology in Parkinson's disease dementia. *Acta Neuropathol Commun*. 2020;8(1):211–020. -01083-5.
90. Hovens IB, Nyakas C, Schoemaker RG. A novel method for evaluating microglial activation using ionized calcium-binding adapter protein-1 staining: cell body to cell size ratio. *Neuroimmunol Neuroinflammation*. 2014;1(2):82–8.
91. Shapiro LA, Perez ZD, Foresti ML, Arisi GM, Ribak CE. Morphological and ultrastructural features of Iba1-immunolabeled microglial cells in the hippocampal dentate gyrus. *Brain Res*. 2009;1266:29–36.
92. Wennersten A, Holmin S, Al Nimer F, Meijer X, Wahlberg LU, Mathiesen T. Sustained survival of xenografted human neural stem/progenitor cells in experimental brain trauma despite discontinuation of immunosuppression. *Exp Neurol*. 2006;199(2):339–47.
93. Tam RY, Fuehrmann T, Mitrousis N, Shoichet MS. Regenerative therapies for central nervous system diseases: a biomaterials approach. *Neuropsychopharmacology*. 2014;39(1):169–88.
94. Falk T, Gonzalez RT, Sherman SJ. The Yin and Yang of VEGF and PEDF: multifaceted neurotrophic factors and their potential in the treatment of Parkinson's Disease. *Int J Mol Sci*. 2010;11(8):2875–900.
95. Tsukahara T, Takeda M, Shimohama S, Ohara O, Hashimoto N. Effects of brain-derived neurotrophic factor on 1-methyl-4-phenyl-1,2,3,6-tetrahydropyridine-induced parkinsonism in monkeys. *Neurosurgery*. 1995;37(4):733–9. discussion 739–41.
96. Hirsch MA, van Wegen EEH, Newman MA, Heyn PC. Exercise-induced increase in brain-derived neurotrophic factor in human Parkinson's disease: a systematic review and meta-analysis. *Transl Neurodegener*. 2018;7:7-018-0112-1. eCollection 2018.
97. Real CC, Ferreira AF, Chaves-Kirsten GP, Torrao AS, Pires RS, Britto LR. BDNF receptor blockade hinders the beneficial effects of exercise in a rat model of Parkinson's disease. *Neuroscience*. 2013;237:118–29.
98. van den Berge SA, van Strien ME, Hol EM. Resident adult neural stem cells in Parkinson's disease—the brain's own repair system? *Eur J Pharmacol*. 2013;719(1–3):117–27.
99. Thome AD, Standaert DG, Harms AS. Fractalkine Signaling regulates the inflammatory response in an alpha-synuclein model of Parkinson Disease. *PLoS ONE*. 2015;10(10):e0140566.
100. Akerud P, Canals JM, Snyder EY, Arenas E. Neuroprotection through delivery of glial cell line-derived neurotrophic factor by neural stem cells in a mouse model of Parkinson's disease. *J Neurosci*. 2001;21(20):8108–18.
101. Fox CM, Gash DM, Smoot MK, Cass WA. Neuroprotective effects of GDNF against 6-OHDA in young and aged rats. *Brain Res*. 2001;896(1–2):56–63.
102. Perez-Bouza A, Di Santo S, Seiler S, Meyer M, Anderegg L, Huber A, et al. Simultaneous transplantation of fetal ventral mesencephalic tissue and encapsulated genetically modified cells releasing GDNF in a Hemi-Parkinsonian Rat Model of Parkinson's Disease. *Cell Transpl*. 2017;26(9):1572–81.
103. Brigadski T, Leßmann V. The physiology of regulated BDNF release. *Cell Tissue Res*. 2020;382(1):15–45.
104. Fernández-García S, Sancho-Balsells A, Longueville S, Hervé D, Guart A, Delgado-García JM, et al. Astrocytic BDNF and TrkB regulate severity and neuronal activity in mouse models of temporal lobe epilepsy. *Cell Death Dis*. 2020;11(6):411–020.
105. Bambah-Mukku D, Travaglia A, Chen DY, Pollonini G, Alberini CM. A positive autoregulatory BDNF feedback loop via C/EBP $\beta$  mediates hippocampal memory consolidation. *J Neurosci*. 2014;34(37):12547–59.
106. Jiang C, Lin WJ, Salton SR. Role of a VGF/BDNF/TrkB Autoregulatory Feedback Loop in Rapid-acting antidepressant efficacy. *J Mol Neurosci*. 2019;68(3):504–9.

## Publisher's note

Springer Nature remains neutral with regard to jurisdictional claims in published maps and institutional affiliations.